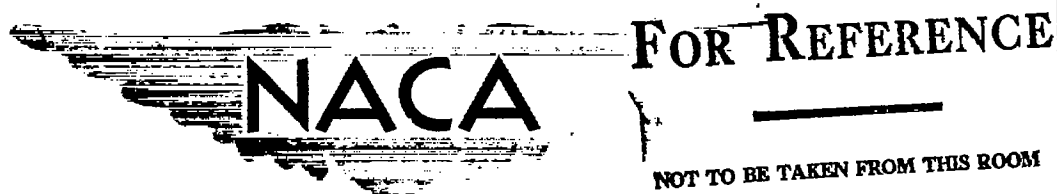


UNCLASSIFIED  
SECURITY INFORMATION

3 1176 00150 3128

Copy 151  
RM E52119



# RESEARCH MEMORANDUM

THE SODIUM HYDROXIDE REACTOR: EFFECT OF REACTOR  
VARIABLES ON CRITICALITY AND FUEL-ELEMENT  
TEMPERATURE REQUIREMENTS FOR SUBSONIC  
AND SUPERSONIC AIRCRAFT NUCLEAR

PROPELLION

By Donald Bogart and Michael F. Valerino

11. 00-1596  
JUN 20 1955

Lewis Flight Propulsion Laboratory  
Cleveland, Ohio

CLASSIFICATION CHANGED  
UNCLASSIFIED

To

By authority of CEN-2121 dtd: Date  
Mar. 31, 1971

~~RESTRICTED DATA~~

LIBRARY COPY

~~THIS DOCUMENT CONTAINS RESTRICTED  
DATA AS DEFINED IN THE ATOMIC ENERGY  
ACT OF 1946. ITS TRANSMISSION OR DIS-  
CLOSURE OR ITS CONTENTS IN ANY MANNER  
TO AN UNAUTHORIZED PERSON IS PRO-  
HIBITED. CLASSIFIED DOCUMENT~~

NOV 15 1971

LANGLEY RESEARCH CENTER

LIBRARY, NASA

This material contains information affecting the National Defense of the United States within the meaning  
of the espionage laws, Title 18, U.S.C., Secs. 793 and 794, the transmission or revelation of which in any  
manner to unauthorized person is prohibited by law.

NATIONAL ADVISORY COMMITTEE  
FOR AERONAUTICS

WASHINGTON

FEB 10 1955

~~REDACTED~~ UNCLASSIFIED

**SECURITY INFORMATION**

NACA RM E52I19

~~SECRET~~THIS DOCUMENT CONSISTS OF.....<sup>84</sup> PAGES

NO. 151 OF 160 COPIES, SERIES B

**UNCLASSIFIED**  
NATIONAL ADVISORY COMMITTEE FOR AERONAUTICSRESEARCH MEMORANDUMTHE SODIUM HYDROXIDE REACTOR: EFFECT OF REACTOR VARIABLES ON CRITICALITY  
AND FUEL-ELEMENT TEMPERATURE REQUIREMENTS FOR SUBSONIC AND  
SUPERSONIC AIRCRAFT NUCLEAR PROPULSION

By Donald Bogart and Michael F. Valerino

## SUMMARY

Results are presented of two-group criticality calculations made for sodium-hydroxide-cooled, moderated, and reflected reactors for various concentrations and compositions of reactor fuel-element structural material. These specific criticality results are presented in a generalized manner to permit rapid evaluation of the criticality requirements for a wide range of other structural material compositions and concentrations which may be of interest from considerations of corrosion, strength, and heat-transfer-surface requirements.

Based on turbojet-engine cycle operating conditions optimized for minimum airplane gross weight, the maximum reactor fuel-element and coolant temperatures are related to the reactor heat release and airplane gross weight for a range of the reactor heat-transfer variables for flight at altitudes of 30,000 and 50,000 feet and Mach numbers of 0.9 and 1.5. For the calculations, airplane lift-drag ratio is assumed constant at 6.5 for supersonic and 18 for subsonic flight. The weight of shield plus reactor plus payload plus auxiliaries (herein designated as  $W_K$ ) is assumed constant at two different values namely, 100,000 and 150,000 pounds; the calculated results for 100,000 pounds are considered representative for the divided-type shadow shield, the results for 150,000 pounds apply for the unit bulk shield.

The results provide a basis for compromise of the advantages of higher cycle efficiencies (and hence lower airplane gross weights, reactor heat releases, and engine air flows) attainable at high reactor fuel-element temperatures with the advantages of higher reactor-material strength and corrosion resistance attainable at low fuel-element temperatures.

For subsonic flight at altitudes of 30,000 and 50,000 feet and for values of  $W_K$  of 100,000 and 150,000 pounds, maximum reactor fuel-element temperatures of the order  $1100^{\circ}$  to  $1200^{\circ}$  F can be maintained with a reactor core diameter of 2 feet. The airplane gross weight and reactor heat

~~RESTRICTED DATA~~~~SECRET~~  
THIS DOCUMENT CONTAINS RESTRICTED DATA AS DEFINED IN THE ATOMIC ENERGY ACT OF 1946. ITS TRANSMISSION OR DISCLOSURE OF ITS CONTENTS IN ANY MANNER TO AN UNAUTHORIZED PERSON IS PROHIBITED.**UNCLASSIFIED**

2525

release are approximately 200,000 pounds and 70,000 kilowatts, respectively, for  $W_K$  of 100,000 pounds and are proportionately increased to approximately 300,000 pounds and 100,000 kilowatts, respectively, for  $W_K$  of 150,000 pounds.

Supersonic flight at a 30,000-foot altitude increases maximum reactor fuel-element temperatures to the  $1200^{\circ}$  to  $1300^{\circ}$  F range for approximately the same values of airplane gross weight as required for subsonic flight; reactor heat releases required, however, are about four times greater than for subsonic flight.

Supersonic flight at 50,000 feet altitude requires maximum reactor fuel-element temperatures to increase to the  $1300^{\circ}$  to  $1500^{\circ}$  F range for  $W_K$  of 100,000 pounds, and to the  $1400^{\circ}$  to  $1600^{\circ}$  F range for  $W_K$  of 150,000 pounds for a reactor core diameter of 2 feet. For this flight condition, reduction in maximum fuel-element temperature to the  $1100^{\circ}$  to  $1200^{\circ}$  F level for  $W_K$  of 100,000 pounds, and to the  $1200^{\circ}$  to  $1300^{\circ}$  F level for  $W_K$  of 150,000 pounds, can be achieved by an increase in reactor core diameter to 2.5 feet. Airplane gross weight and reactor heat release are then 300,000 pounds and 350,000 kilowatts, respectively, for  $W_K$  of 100,000 pounds and are proportionately larger for  $W_K$  of 150,000 pounds.

Enriched uranium investments for the hot unpoisoned reflected reactor, containing sufficient high-nickel-alloy fuel elements to provide appropriate heat-transfer surface for the aforementioned reactor and airplane flight conditions, are of the order of 35 and 50 pounds for core diameters of 2.0 and 2.5 feet, respectively. As fuel-element structural material in the reactor is reduced to zero concentration, the uranium investments approach 15 and 20 pounds for the 2.0- and 2.5-foot core diameters, respectively. The excess uranium required to counteract burnup and the poisoning effects of equilibrium xenon, samarium, and other fission products resulting from reactor operation for 24 hours at 300,000 kilowatts is estimated to be less than 10 pounds. At this poisoned condition, the temperature coefficient of reactivity for reactors with high-nickel-alloy fuel elements was calculated to be negative and of the order of -0.00006 per  $^{\circ}$ F.

#### INTRODUCTION

Reactors cooled and moderated by liquid hydroxides, with uranium either contained in fixed structural elements or present in compound form as a slurry in the hydroxide, have many attractive features to warrant detailed investigation of their applicability to aircraft nuclear propulsion. The high effectiveness of the hydroxides in slowing down neutrons makes for relatively small reactor sizes and hence small shield weights, which is particularly essential in aircraft application. The use of hydroxides, in functioning as combined coolant-moderator, leads to less

complicated reactor core structures compared with the air-cooled or liquid-metal-cooled reactors which require incorporation of a separate moderator into the reactor. No pressurization is required to keep the hydroxides in the liquid state at the operating temperatures required for the aircraft application; in addition, the hydroxides maintain reasonably high densities at these temperatures. These two characteristics represent important advantages over the use of water as a coolant-moderator.

Important disadvantages in the use of the hydroxides are associated with: (a) their relatively low heat-transfer coefficients as compared with the liquid metals; (b) their high melting points; (c) their susceptibility to radiation decomposition; (d) their corrosive action on the available materials having the high-temperature strength required in the reactor and reactor coolant loop.

The inferior heat-transfer ability of the hydroxides compared with the liquid metals is partly compensated by the greater reactor coolant-flow area and fuel-element heat-transfer surface area attainable with the hydroxides due to absence of a fixed moderator. Lower heat fluxes can therefore be attained in the hydroxide reactors so that temperature differentials between fuel element and coolant for the hydroxide case can be made to approach that for the liquid-metal-cooled reactor.

Because of the high melting points of the hydroxides, the procedure for filling and for draining the reactor coolant requires prior heating of the reactor and loop, which introduces complications in starting up and shutting down the nuclear power plant.

Whether radiation decomposition of the hydroxides at the operating conditions is an important enough consideration to rule out the hydroxides as possible reactor coolant-moderator remains unanswered at this time. Experience with water at high temperatures and pressures, has indicated that decomposition is much less severe than previously believed because of the high rates of recombination. Because the same mechanisms for recombination are operative for the hydroxides, this fact is encouraging.

The major problem in the use of the hydroxides is the development of materials possessing both high-temperature strength and corrosion resistance to the hydroxides. Inasmuch as strength and corrosion-resistant properties of materials become progressively poorer with increases in temperature, it is advantageous to operate at the lowest fuel-element temperatures consistent with the requirements of reasonable reactor total heat releases and airplane gross weights.

It is the purpose of this report to establish whether the hydroxide reactor shows sufficient promise for aircraft application from the stand-point of: (1) achieving small reactor sizes with reasonable fissionable material investments; and (2) providing required reactor heat releases at

required coolant temperatures without the necessity of excessive fuel-element temperatures. The investigation was conducted at the NACA Lewis laboratory.

Some evaluation work of the sodium hydroxide reactor for aircraft propulsion has been made in references 1 to 3. Of the common hydroxides, sodium hydroxide has been generally selected because of its relatively low melting point and its satisfactory neutron absorption properties.

Reference 1 is concerned with a low-powered stationary reactor intended to serve as a step in the approach to the high-power reactor. In reference 2 a general design and performance study is made of a nuclear-powered subsonic airplane having a homogeneous sodium hydroxide reactor (reactor in which the uranium is assumed as being dissolved or present as a slurry in the hydroxide). The study points up many of the practical problems involved in a hydroxide reactor power-plant system. In reference 3 a brief study is made of a sodium hydroxide reactor with fixed fuel elements. The results indicate that the sodium hydroxide reactor with fixed fuel elements is sufficiently promising for subsonic aircraft propulsion (Mach number, 0.8) to justify developmental work.

In the present report more extensive exploratory calculations are made of the criticality and heat-transfer characteristics of the sodium-hydroxide-cooled and moderated reactor with fixed fuel elements. The calculation results provide:

(a) A generalized chart permitting rapid engineering evaluation of criticality requirements for reflected sodium hydroxide reactors incorporating structural materials of a wide range of compositions and concentrations.

(b) An evaluation of maximum reactor fuel-element temperatures, for a range of reactor heat-transfer variables, necessary to satisfy the power requirements corresponding to both subsonic and supersonic aircraft propulsion.

(c) A basis for compromise of the advantages of higher turbojet cycle efficiencies resulting from operation at high fuel-element temperatures with the advantages of higher structural-material strength and corrosion resistance resulting from operation at low fuel-element temperatures.

(d) An indication of the temperature coefficients of reactivity and excess uranium requirements corresponding to equilibrium fission-product poisoning for several reactor assemblies of interest.

## SCOPE OF INVESTIGATION OF REACTIVITY VARIABLES

2525 The reactor core is taken as a right circular cylinder of length-diameter ratio equal to unity. Fissionable material is contained within tubes or plates over which the sodium hydroxide NaOH flows to pick up the fission heat generated within the fissionable material. The core is reflected by routing of NaOH around the core prior to its passing through the core, as schematically indicated in figure 1. The composition of the reactor core is primarily NaOH with a relatively small volume of structural material containing fissionable material and possibly a diluent, or carrier, for the fissionable material.

## Criticality Calculations

Reactor size and uranium investment are dependent, to a large extent, on the amount and composition of the structural material present in the reactor core. At present, however, no structural material is known that is satisfactorily resistant to corrosion by NaOH at the temperatures required for the aircraft application. Hence, no definite assignment of structural material composition can be made for a specific evaluation of the NaOH-cooled and moderated reactor.

As indicated in the section under "Method of Generalization of Criticality Results", reactor criticality requirements are influenced by structural material content principally through two quantities: the macroscopic thermal absorption cross section of the structure  $\Sigma_{A,th}^s$  and the reactor volume fraction of structure  $f_s$ . For convenience, the macroscopic cross section  $\Sigma_{A,th}^s$  is put on a unit reactor volume basis and is hereafter referred to as the thermal absorption parameter  $f_s \Sigma_{A,th}^s$ . (Symbols are defined in appendix A.) The effect of variation of  $f_s$  on criticality is determined on the basis of theoretical considerations. The effect of  $f_s \Sigma_{A,th}^s$  for a given  $f_s$  must be determined by detailed criticality calculations made for several structural-material compositions and concentrations. By means of these parameters, criticality results for specific structural material contents in the reactor can be plotted in a generalized manner to be applicable for a wide variety of other structural material compositions and concentrations.

The following specific reactor-core compositions were chosen for the criticality calculations to provide the basic data required for mapping the criticality characteristics of the family of NaOH-cooled and moderated reactors over a suitably large range of values of the thermal absorption parameter  $f_s \Sigma_{A,th}^s$ .

Reactor	Composition by volume				$f_s$	$f_s \Sigma_{A,th}^s$
	NaOH	Ni	Fe	Na		
I	0.82	0.08	--	0.10	0.08	0.0151
II	.82	--	0.08	.10	0.08	0.0074
III	.90	--	--	.10	0	0
IV	1.00	--	--	--	0	0

2525

For these reactors, a wide range of uranium U concentration, corresponding to ratios of H to  $U^{235}$  atoms R from 50 to 500, were investigated. The reactor fission spectrum ranged from thermal to intermediate (fast-fission contributions from 10 to 50 percent of the total). Various thicknesses of NaOH reflector from zero to effectively infinite were investigated. Reflector effects were measured by the two-group reflector savings, defined as the difference between the unreflected and the reflected reactor-core radii.

In reactors I and II, structural material content is taken as 8 percent by volume of Ni and Fe, respectively. Nuclear properties of these metals bracket the properties of a large number of high-temperature alloys and ceramics considered to be satisfactory, nuclearwise, for use in aircraft reactors. The 8-percent concentration of these metals is sufficiently high to provide for a fuel-element design and auxiliary structure having adequate heat-transfer surface for a reactor of the order of 300,000-kilowatt output. Metallic Na is included in the reactor as representative, nuclearwise, of the fissionable-material diluents or carriers that may be present within the fuel elements. Reactor III represents the limiting case of zero structural material content. Reactor IV provides a comparison of the effect of the Na additive on reactor criticality and represents the truly homogeneous reactor type.

Two-group neutron diffusion theory was employed in the criticality calculations. Spherical geometry was assumed in the reflected reactor calculations and a transformation made to cylindrical geometry under the assumption that the reflector savings remain the same. The derivation and method of solution of the two-group equations are briefly reviewed in appendix B. The evaluation of the gross nuclear constants required in the use of the two-group theory equations is briefly described in the following section "Evaluation of Nuclear Constants" and is presented in detail in appendix C.

Results of the criticality calculations are presented in the following manner:

(1) For reactors I to IV, curves of the enriched uranium investment as a function of reactor core diameter are presented for various reflector thicknesses.

(2) Reflector savings for these reactors are compared.

(3) Representative neutron flux and power generation distributions for reactors I and III are presented.

(4) For the generalized family of NaOH reactors, a chart of uranium investment as a function of the thermal absorption parameter  $f_s \Sigma_{A,th}^S$  is presented for various reactor diameters and values of  $f_s$ .

#### Evaluation of Nuclear Constants

Validity of the two-group representation used here depends entirely on the correctness of the nuclear constants used to represent, in a bulk fashion, the various competing nuclear processes occurring within the two neutron-energy groups. In order to reduce the uncertainties involved in the evaluation of these bulk nuclear constants, the procedure used is patterned, as closely as possible, after that successfully used in reference 4 to predict the criticality of small hydrogen-moderated (water, in this case) thermal reactors. The procedure for evaluating the constants, which is described in detail in appendix C, is briefly outlined as follows:

$\lambda_{TR,f}$ ,  $\Sigma_{A,f}$ ,  $\Sigma_{F,f}$ ,  $p_{th}$ . - The constants  $\lambda_{TR,f}$ ,  $\Sigma_{A,f}$ ,  $\Sigma_{F,f}$ , and  $p_{th}$  are obtained by weighting local values according to the energy distribution of neutron flux in an infinite medium of the same composition, as indicated by age theory. The fission neutron-energy spectrum (taken from reference 5) is included in determining the energy distribution.

$L_f^2$ . - The solution of the transport equation for the second moment of the spatial distribution of neutrons slowing down from a point source in an infinite medium consisting of a mixture of hydrogen and heavy elements, as derived in reference 6, is used to determine  $L_f^2$ . From the solution of reference 6,  $L_f^2$  is obtained as a function of fission energy and is then weighted over the fission neutron-energy spectrum. The calculations are normalized (see appendix C) to the experimentally determined value of  $L_f^2$ , for water at room temperature, of 33 square centimeters. The value of  $L_f^2$  thus obtained assumes no neutron absorption during slowing down; for the reactors under consideration, however, significant absorption occurs in the energy range from about 1000 ev to thermal. Inasmuch as the slowing-down process in this energy range can be considered continuous, age theory is approximately applicable and hence is used to estimate the effect of absorption on slowing down in this energy range. The difference in age with and without absorption in

the energy range 1000 ev to thermal was calculated and found to be negligible. On this basis and, in addition, because the bulk of the  $L^2_f$  contribution is due to the slowing down in the energy range above 1000 ev, the effect of absorption on  $L^2_f$  is taken to be negligible for the reactors under consideration. (The effect of absorption in the fast group on criticality is hence accounted for solely through its effect on  $P_{th}$ ).

$\lambda_{TR,th}$ . - The method of reference 7 for estimating the effect of chemical binding on thermal neutron diffusion in a hydrogenous medium is used to evaluate  $\lambda_{TR,th}$ . In this method the experimentally determined variation of scattering cross section  $\sigma_s$  with neutron energy for hydrogen (as measured for water, reference 8) is used to obtain  $\lambda_{TR}$  as a function of neutron energy. The assumption involved here is that the chemical bond of H in NaOH is the same as that in water. The value of  $\lambda_{TR,th}$  is then obtained by weighting  $\lambda_{TR}$  according to the flux of neutrons in a Maxwellian distribution corresponding to the moderator temperature.

$\Sigma_{A,th}$ ,  $\Sigma_{F,th}$ . - Local values of  $\Sigma_A$  and  $\Sigma_F$  are assumed to vary with neutron energy according to  $1/v$  in the vicinity of thermal energy;  $\Sigma_{A,th}$  and  $\Sigma_{F,th}$  are then obtained by weighting  $\Sigma_A$  and  $\Sigma_F$ , respectively, according to the flux of neutrons in a Maxwellian distribution corresponding to the moderator temperature.

The constants  $K_F$ ,  $K_{th}$ , and  $L^2_{th}$  are then given by:

$$K_F = \frac{v\Sigma_{F,f}}{\Sigma_{A,f}} ; K_{th} = \frac{v\Sigma_{F,th}}{\Sigma_{A,th}} ; L^2_{th} = \frac{\lambda_{TR,th}}{3\Sigma_{A,th}}$$

In the criticality calculations, the average temperature of the NaOH moderator is taken equal to  $1450^{\circ}$  F ( $E_{th} = 0.092$  ev). In all the reactors, the constituents of the reactor core are assumed to be completely intermixed so that the criticality calculation results do not include any self-shielding effects arising from any heterogeneity of the reactor composition. The fuel cross-section data were taken from measurements on K-25 end product consisting of 91.5 percent  $U^{235}$ , 1.5 percent  $U^{234}$ , and 7.0 percent  $U^{238}$  normalized per atom of  $U^{235}$ . Densities of the materials in the reactor (at  $1450^{\circ}$  F average temperature) are tabulated in table I.

A summary of two-group constants for the specific reactors analyzed in the present study is presented in table II.

## Calculations of Temperature Coefficient of Reactivity

## and Excess Uranium Requirement

In order to provide an indication of the static stability characteristics of NaOH-cooled and moderated reactors, two-group perturbation theory was used to calculate the temperature coefficient of reactivity for the following cases:

Reactor I:  $R = 100$  and  $200$ ,  $t_r = 6$  inches

Reactor III:  $R = 100$  and  $400$ ,  $t_r = 6$  inches

First-order perturbation formulas, modified to include the effect of fast fission, are presented in appendix D.

Calculations were made for the hot reactor with equilibrium  $Xe^{135}$  and 24-hour  $Sm^{149}$  and other fission-product poison concentrations corresponding to reactor operation at 300,000 kilowatts; these concentrations were determined on the basis of information presented in references 9 and 10. The poisons are assumed to be distributed uniformly over the reactor-core volume.

Contributions to the temperature coefficient of reactivity included herein arise from: (1) The change in neutron energy range constituting the fast group, (2) the change in density of NaOH (and hence in atom density of Na, O, and H), and (3) the change in thermal microscopic cross-sections.

The linear variation of density of NaOH with temperature was taken from reference 11. With the exception of  $Xe^{135}$  and  $Sm^{149}$ , absorption and fission microscopic cross-sections in the vicinity of thermal energy are assumed to follow the  $1/v$  law. The variation of microscopic absorption cross-section of  $Xe^{135}$  with temperature, as averaged over the Maxwellian distribution, is obtained from reference 9. The variation of microscopic thermal cross-section of  $Sm^{149}$  with temperature (which contribution to temperature coefficient of reactivity is small relative to the  $Xe^{135}$  contribution) was estimated on the basis of the data of reference 10.

Appendix D presents the perturbation formula and procedure for obtaining the adjoint functions used in the formula; the perturbation formula presented is an extension of that derived in reference 12 to include the effects of fast fission. Appendix D also presents details of the method of evaluation of the various weighting factors contributing to the temperature coefficient of reactivity.

In addition to determination of temperature coefficient of reactivity, two-group perturbation theory was used to estimate the

excess fissionable material required to compensate for burn-up and equilibrium fission-product poisoning for the same reactors. Although the principal poisons are  $Xe^{135}$  and  $Sr^{90}$ , a host of other fission fragment poisons appear and are accounted for by the assumption that for every uranium atom fissioned, the equivalent of a single atom appears having a microscopic absorption cross section of 100 barns at 0.025 ev. The details of the method of calculation are outlined in appendix D. The results of the aforementioned calculations are presented in tabular form.

2525

#### Method of Generalization of Criticality Results

For the range of NaOH reactor compositions of interest for aircraft, the principal contribution to neutron slowing-down and diffusion processes is made by the NaOH, whereas the principal contribution to the absorption process is made by the structural material and uranium. For engineering evaluations, therefore, it may be assumed that the over-all scattering and slowing-down in the reactor core are relatively unaffected by variation in concentration and composition of structural material from the values assumed for specific reactors I to IV.

Therefore, the only two important effects on reactor criticality requirements due to variation in structural material composition and concentration in the reactor are: (a) the effect of neutron absorption by the structural material, which is given by the thermal absorption parameter  $f_s \Sigma_{A,th}^s$  for a  $1/v$  absorber, and (b) the effect of displacement of NaOH moderator by the structural material when volume concentrations  $f_s$  differ from the values assumed for the specific reactors.

Variation in  $f_s$  about a reference value can be treated as equivalent to the effect of void space; a decrease in structural-material volume from the reference value is equivalent to the removal of void space by the same amount; an increase in structural-material volume from the reference value is equivalent to displacement of moderator by the same amount. The effect of void space on reactor size and uranium investment, that is, the effect of  $f_s$ , is treated in appendix B.

As previously mentioned, the effect of  $f_s \Sigma_{A,th}^s$  is obtained from specific criticality calculations in which  $f_s \Sigma_{A,th}^s$  is varied over the range of interest. For a mixture of elements, the parameter  $f_s \Sigma_{A,th}^s$  is given by:

$$f_s \Sigma_{A,th}^s = f_s (c_1 \Sigma_{A,1} + c_2 \Sigma_{A,2} + \dots + c_n \Sigma_{A,n}) \quad (1)$$

where  $c$  is the fraction by volume of elements in structure.

2525

In table III are listed representative alloying elements which may be employed. These absorbers follow the  $1/v$  law in the thermal region with little probability of strongly absorptive, low-lying resonances being present (see reference 13). Therefore the generalization may also be used to evaluate criticality requirements for NaOH reactors containing materials other than Ni and Fe and for a range of volume concentration.

Although the generalization is not strictly rigorous in that it neglects the small differences in neutron slowing-down properties due to other structural materials, it does account for the important first-order effects provided:

- (1) The neutron absorption cross section of the structural material varies with neutron velocity according to  $1/v$  at least up to energies of the order of 100 electron volts.
- (2) The volume of structural material in the reactor is small compared with the volume of moderator.

#### SCOPE OF INVESTIGATION OF PERFORMANCE OF NUCLEAR-POWERED AIRCRAFT

The purpose of this performance study is to determine the airplane gross weight and reactor heat-release requirements as affected by the maximum temperature of the reactor fuel elements for a range of reactor and reactor heat-transfer variables for various airplane flight conditions.

The turbojet cycle, involving a tertiary system of two separate closed liquid circuits and an open air cycle, is used in the study of the performance of a nuclear-powered aircraft utilizing the NaOH reactor as the heat source. A schematic diagram of this cycle is shown in figure 2. In the primary liquid circuit, NaOH is heated as it flows through the reactor and then cooled as it flows through the primary heat exchanger where it gives up its heat to a liquid metal flowing in the secondary liquid circuit. In the secondary circuit, heat picked up by the liquid metal is transferred to the air in the secondary heat exchanger.

Air enters the diffuser of the turbojet engine, is compressed by a compressor, is heated in the secondary heat exchanger, and is expanded through a turbine which extracts sufficient energy from the high-pressure, high-temperature air to run the compressor. Finally the air expands through an exhaust nozzle into the atmosphere to provide the propulsive jet thrust.

The configuration of reactor fuel elements chosen for determination of heat-transfer characteristics of the NaOH reactor is shown schematically in figure 1. This configuration was chosen for convenience in the heat-transfer study intended to indicate what may be accomplished

with respect to heat transfer in the NaOH reactor; no detailed study of the structural, mechanical, or fabrication problems associated with various core designs was made in arriving at the configuration chosen.

As indicated in figure 1, the fuel elements are considered to be plates of sandwich-type construction arranged in a closely spaced parallel array within the reactor core. NaOH flows in a single pass between the plates from one face of the cylindrical core through to the opposite face. (Choice of small-diameter tubes instead of plates would give approximately the same heat-transfer results.)

2525

#### Reactor Heat Transfer

In the heat-transfer study, the maximum temperature of the fuel-element plates corresponding to any value of total reactor heat release and reactor-exit coolant temperature is related to the variables: reactor core diameter  $D_c$  (note,  $L_c = D_c$ ), fraction of core volume occupied by fuel-element material  $f_s$ , fuel-element plate thickness  $t_p$ , and coolant velocity  $V$ .

Two methods of reactor operation have been assumed: (1) uniform heat generation over entire reactor-core volume, and (2) uniform fuel-element wall temperature.

Basic relations and procedure used in the heat-transfer study are outlined as follows:

(1) From geometrical considerations, the plate spacing  $s_p$ , area for coolant flow  $A$ , and heat-transfer surface area  $S$  are obtained for assigned reactor core size  $D_c$ , percent of core volume occupied by fuel-element material  $f_s$ , and plate thickness  $t_p$ .

(2) The heat-transfer coefficient  $h$  corresponding to a given coolant velocity  $V$  is then obtained by use of the Nusselt relation

$$\frac{h D_e}{k} = 0.023 \left( \frac{\rho V D_e}{\mu} \right)^{0.8} \left( \frac{c_p \mu}{k} \right)^{0.4}$$

where  $D_e = 2 s_p$ .

The physical properties for the NaOH coolant employed in the present calculations are as follows:

Density, $\rho$ , lb/cu ft . . . . .	98.0
Specific heat, $c_p$ , Btu/lb-°F . . . . .	0.483
Viscosity, $\mu$ , lb/hr-ft . . . . .	2.5
Conductivity, $k$ , Btu/(hr)(sq ft)(°F/ft). . . . .	0.68

Density data were taken from reference 11. Viscosity, specific heat, and thermal conductivity of NaOH were obtained from data transmitted from Battelle Memorial Institute.

(3) For the case of constant rate of heat input along a flow passage, the temperature differential between the passage wall and coolant is constant along the flow passage (for constant  $h$  along passage). Hence the heat balance may be expressed as:

$$H = hS (T_{w,ex}^0 - T_{c,ex}) = \rho AV c_p (T_{c,ex} - T_{c,en})$$

from which the ratios  $\frac{T_{w,ex}^0 - T_{c,av}}{H}$  and  $\frac{T_{c,ex} - T_{c,av}}{H}$  are readily

determined. The temperature differences are expressed per kilowatt of heat release in order to make the heat-transfer results general for any value of reactor heat release.

(4) For the case of uniform wall temperature, the temperature differential between the passage wall and coolant varies along the flow passage. The heat balance for this case is written as:

$$H = hS \frac{(T_{c,ex} - T_{c,en})}{\log_e \left( \frac{T_{w,ex}^0 - T_{c,en}}{T_{w,ex}^0 - T_{c,ex}} \right)} = \rho AV c_p (T_{c,ex} - T_{c,en})$$

from which the ratios  $\frac{T_{w,ex}^0 - T_{c,av}}{H}$  and  $\frac{T_{c,ex} - T_{c,av}}{H}$  are determined.

(5) The temperature drop across the fuel-element plate is calculated by use of the heat-conduction equation  $H/S = -k_s \frac{T_{w,ex}^0 - T_{w,ex}}{t_p/2}$ , assuming all the heat is generated at the center line of the plate cross section. The following relation can then be obtained:

$$\frac{T_{w,ex} - T_{c,av}}{H} = \frac{T_{w,ex}^0 - T_{c,av}}{H} + \frac{t_p}{2k_s S}$$

The thermal conductivity of the fuel plates used in calculation of temperature drop across the plates is taken as 28 Btu/(hr)(sq ft)(°F/ft) the value for nickel at 1500° F. The thermal conductivity for carbon, stainless, and high-alloy steels is about 15 Btu/(hr)(sq ft)(°F/ft). (reference 15). Inasmuch as the temperature drop across the fuel plates, for the conditions considered, is generally less than 10 percent of the over-all drop to the average coolant temperature, variation in thermal conductivity of the fuel-plate material has not been considered.

The results of the foregoing procedure are presented in the following manner:

For a fixed reactor core size and percent of core volume occupied by fuel-element material,  $\frac{T_w, ex - T_c, av}{H}$  and  $\frac{T_c, ex - T_c, av}{H}$  are plotted against  $V$  (range, 5 to 30 ft/sec) for various fuel plate thicknesses.

Reactor heat-transfer characteristics are presented for the case of uniform heat generation for:

Reactor core diameter, ft . . . . . 2.0, 2.5, 3.0  
 Fuel-element reactor volume fraction . . . . . 0.06, 0.12  
 Fuel-element plate thickness, in. . . . . 0.012, 0.016, 0.020

Comparative heat-transfer characteristics are presented for the case of uniform wall temperature for each of the reactors for a fuel-element-plate thickness of 0.012 inch.

#### Airplane and Turbojet Cycle

The performance study of the turbojet cycle system in a nuclear-powered aircraft is based on the optimized engine performance results of reference 14, wherein the turbojet cycle is optimized to give minimum gross airplane weight  $W_g$  for fixed values of airplane lift-drag ratio  $L/D$ , structure-to-gross-weight ratio  $W_s/W_g$ , and weight of shield, reactor, pay load and auxiliary equipment  $W_K$ . The optimized performance is given by relations between the air heat-exchanger effective wall temperature  $T_{w, eff}$  and values of the following variables: (a) engine thrust per weight of engine plus air heat exchanger  $F_n/W_T$ , (b) net thrust per pound of air per second  $F_n/W_a$ , and (c) heat addition per pound air  $\Delta h_x$ . From these quantities, the airplane gross weight, reactor heat release, and engine air flow are found from the following relations for any value of air heat-exchanger effective wall temperature:

$$W_g = \frac{W_K}{1 - \frac{W_s}{W_g} - \frac{1}{(F_n/W_T)(L/D)}}$$

$$w_a = \frac{W_g}{(L/D)(F_n/w_a)}$$

$$H = w_a \Delta h_x$$

Values of variables selected for the airplane study are:  $W_K$ , 100,000 and 150,000 pounds;  $L/D$  = 6.5 (supersonic) or 18 (subsonic); and  $W_s/W_g$  = 0.30.

The values of  $W_K$  selected are believed to be representative of the divided and unit-type shields contemplated for the nuclear airplane. The values of  $L/D$  selected conform with existing practice for the subsonic case and represent a reasonable value for the supersonic case. The value of  $W_s/W_g$  used conforms with the findings of recent nuclear airplane weight analyses.

#### Maximum Fuel-Element Temperature Evaluation

In order to relate the airplane gross weight and reactor heat release to the maximum temperature of the reactor fuel elements, it is necessary to combine the engine performance and the heat-transfer studies. The procedure used is outlined as follows:

(a) For assigned values of  $W_K$ ,  $L/D$ , and  $W_s/W_g$ , the method outlined in the previous section is used to determine  $W_g$ ,  $w_a$ , and  $H$  for a range of values of  $T_{w,eff}$ .

(b) On the basis of a preliminary primary heat-exchanger design study, the average NaOH coolant temperature within the reactor is taken as  $100^{\circ}$  F higher than  $T_{w,eff}$ , that is,  $T_{c,av} - T_{w,eff} = 100^{\circ}$  F. The heat-exchanger design study indicated that this temperature differential can be easily attained with reasonably small primary heat-exchanger size for reactor heat releases required for supersonic flight conditions.

(c) For assigned values of reactor size, coolant velocity, fuel-element material volume, and fuel-element thickness, the maximum fuel-element temperature is computed by adding the following temperature differences:

$$T_{w,ex} = (T_{w,ex} - T_{c,av}) + (T_{c,av} - T_{w,eff})$$

A schematic diagram of the heat-exchanger system and relative temperature distribution is presented in figure 3. The temperature difference  $T_{w,ex} - T_{c,av}$  is found from the heat-transfer parameter  $\frac{T_{w,ex} - T_{c,av}}{H}$  by multiplying by the value of  $H$  determined in step (a).

## RESULTS AND DISCUSSION

## Specific Reactor Calculations

Criticality calculation results for the core compositions represented by reactors I to IV are presented in figure 4. In these figures, uranium investment is plotted against cylinder core diameter for reflector thicknesses of 0, 3, 6, and 12 inches. (Cylinder length-diameter ratio is taken equal to unity.) In the calculation of these curves for each core composition and reflector thickness, a range of values of atom ratio  $R$  is taken and core diameter and resultant uranium investment for criticality are determined. Lines of constant  $R$  are given on each figure.

The curves for each reactor-core composition indicate a minimum total uranium investment for each reflector thickness; minimum total investment decreases and occurs at progressively smaller core diameters as reflector thickness increases to effectively infinite values.

The existence of a reactor size for minimum total uranium investment may be explained as follows: As uranium concentration (per unit volume) is increased, the neutron leakage tolerable for criticality is increased; a decrease in core diameter results.

At the large core diameters, the neutron leakage is relatively insensitive to diameter so that in order to maintain criticality, a large percentage decrease in core diameter occurs for a small percentage increase in uranium concentration; hence, the total uranium investment, which is proportional to the uranium investment and the cube of the diameter, decreases. At the small core diameters, the neutron leakage is extremely sensitive to diameter and so the opposite effects occur. At some intermediate value of core diameter, the decrease in diameter exactly counteracts the increase in uranium concentration with respect to total uranium investment; this defines the core diameter for minimum investment.

Minimum total uranium investments and corresponding reactor-core diameters for unreflected and reflected reactors are summarized from figure 4 in the following table:

2525

Reactor	Composition by volume				Minimum uranium investment (lb)		Reactor core diameter (ft)	
	NaOH	Ni	Fe	Na	Unreflected	6-in. reflector	Unreflected	6-in. reflector
I	0.82	0.08	--	0.10	93	32	2.7	1.7
II	.82	--	0.08	0.10	69	23	2.7	1.7
III	.90	--	--	0.10	43	13	2.7	1.5
IV	1.00	--	--	--	38	11	2.5	1.5

Considerations of reactor heat transfer and high-altitude supersonic flight power requirements, presented later, indicate that core diameters of the order of 2.5 feet are required to avoid unreasonably high fuel-element temperatures. For a 2.5-foot core diameter and a 6-inch reflector, figure 4 indicates investments of 51, 36, and 21 pounds for reactors I, II, and III, respectively.

#### Reflector Savings

The variation of NaOH reflector savings (defined as the difference between the unreflected and reflected reactor core radii) with reflector thickness for reactors I to IV is presented in figure 5 for representative values of atom ratio  $R$ . Reflector savings increase markedly for reflector thicknesses up to 6 inches, but level off rapidly for larger thicknesses. A line indicating reflector savings equal to reflector thickness is included in figure 5. Reflector savings are about equal to reflector thickness up to thicknesses of 3 inches, indicating no net change in reactor-core radius-plus-reflector thickness; for thicker reflectors, reflector savings are smaller than reflector thickness so that the over-all core-plus-reflector dimensions become larger. From considerations both of over-all size (core plus reflector) and of reflector effectiveness in reducing uranium investment, a reflector thickness of about 6 inches appears to be a satisfactory compromise.

The different reactor core compositions considered herein exhibit approximately the same reflector savings for any given value of reflector thickness. The small effect of increased nonproductive absorber in the core on the reflector savings may be noted in the slightly reduced reflector savings attained for reactors I and II compared with reactors III and IV. Variation of  $R$  in the core also has little effect on the magnitude of reflector savings.

Although the magnitudes of the savings are about the same for thermal reactors (low concentration of uranium) for which core diameters are large, and for intermediate reactors (high concentration of uranium) for which core diameters are relatively small, the savings are much smaller percentages of the core radii for the thermal reactors because the neutron leakage is smaller for thermal reactors.

The curves of figure 4 for the 6-inch NaOH reflector thickness are replotted in figure 6 for convenience of comparison of reactors I to IV. In every case, the reactor core diameters corresponding to minimum investment are less than 2 feet. The curves become steeper on both sides of the minimum investment point as the nonproductive absorption is progressively increased from reactor III to II to I; this steepness is more pronounced in the region of core sizes below that for minimum investment. Inasmuch as the uncertainties introduced by two-group theory become smaller as core size is increased (the value of  $R$  increased with the result that fast-fission contribution was decreased), greater confidence can be placed in the results for core sizes to the right of the minimum investment values.

2525

#### Criticality Generalization

Chart construction. - On the basis of the considerations presented in the section entitled "Methods of Generalization of Criticality Results", the specific results for reactors I, II, and III are replotted to be applicable, in engineering evaluations, to a wide variety of structural-material concentrations and compositions, subject to the restrictions: (a) that the material does not exhibit any large neutron cross-section resonance near thermal energy (below about 100 ev), and (b) that the concentrations must be relatively small (say, less than 16 percent). The generalization, results of which are plotted in figure 7, is accomplished as follows:

A plot (fig. 7(a)) is made of uranium investment  $W^U$  against the thermal absorption parameter  $f_s \Sigma_{A,\text{th}}^s$  for various unreflected reactor core diameters composed as follows:

Volume fraction of structure, . . . . .	.. . . . .	$f_s$
Volume fraction of NaOH plus Na, . . . . .	.. . . . .	$1 - f_s$
Na/NaOH volume ratio, . . . . .	.. . . . .	0.122

The specific results for reactors I, II, and III are used in the construction of this plot employing a reference value of  $f_s$  of 0.08. For reactors I and II, the value of  $f_s$  is 0.08 and so the results are directly applicable; for reactor III,  $f_s$  is zero so that a void correction to  $f_s$  of 0.08 was made by the method discussed in appendix B.

The unreflected core diameters indicated on figure 7(a) are referred to as the chart diameters  $\left(\frac{1-f_s}{0.92}\right) D_c$ . The slant lines on the left of this plot yield the unreflected reactor total uranium investments  $W^U$  for any assigned value of  $f_s$ .

The insert plot (fig. 7(b)) indicates the reduction in core diameter possible with various thicknesses of NaOH reflector. The reduction in core diameter is equal to twice the reflector savings as presented in figure 5; inasmuch as reflector savings are relatively insensitive to core composition, average values were selected for figure 7(b).

Therefore, for assigned values of  $f_s$  and  $D_c$  of interest, figure 7(a) enables determination of enriched uranium investments for the unreflected reactors for any value of  $f_s \Sigma_{A,th}^s$ . Figure 7(b) permits the evaluation of the reflected core diameter for any value of reflector thickness; the uranium investment for reflected reactors, which is proportional to the cube of the core diameter, may be calculated from the uranium investment for the unreflected core.

Chart procedure. - The procedure for using the chart is given by the following steps:

1. A reflected NaOH reactor with actual structural material concentration  $f_s$  and core diameter  $D_c(t_r)$  is assigned.
2. Figure 7(b) gives the reduction in reactor diameter due to NaOH reflectors of various thickness; the unreflected core diameter of interest is then evaluated.

$$D_c = D_c(t_r) + \Delta D_c(t_r)$$

3. The unreflected chart reactor diameter  $\left(\frac{1-f_s}{0.92}\right) D_c$  is calculated by means of the actual value of  $f_s$  and the unreflected core diameter of interest  $D_c$ .

4. Figure 7(a) yields a value of uranium investment  $W^U$  for the unreflected reactor with the actual value of  $f_s$ .

5. The uranium investment for the reflected reactor of interest is then computed.

$$W^U(t_r) = W^U \left[ \frac{D_c(t_r)}{D_c} \right]^3$$

The use of the chart can best be illustrated by an example:

Example. - It is desired to find the enriched uranium investment for a cylindrical reactor of length-diameter ratio of unity, moderated by NaOH (with small percentage of Na additive) and reflected by a 6-inch thickness of NaOH. The reactor core is 2.5 feet in diameter and is to contain volume concentrations of Inconel of (a) 8 percent, and (b) 12 percent. The thermal absorption parameter  $f_s \Sigma_{A,th}^s$  is evaluated for each case in the following table by equation (1):

Element	Fraction by weight	Fraction by volume <sub>c</sub>	$\Sigma_{A,th}^s$ (from table III)	<sup>c</sup> $\Sigma_{A,th}^s$	Case a $f_s \Sigma_{A,th}^s$	Case b $f_s \Sigma_{A,th}^s$
Ni	0.78	0.74	0.189	0.140	0.08 x 0.159	0.12 x 0.159
Fe	.08	.09	.093	.001		
Cr	.14	.17	.103	.018		
Total	1.00	1.00	-----	0.159	0.0127	0.0191

The procedure for using the general criticality results of figure 7 to evaluate the unreflected and reflected reactor core diameter and uranium investments is indicated in the following table:

Case	$f_s$	$f_s \Sigma_{A,th}^s$	$D_c(t_r)$ (ft)	$\Delta D_c$ (ft)	$D_c$ (ft)	$\left(\frac{1-f_s}{0.92}\right) D_c$ (ft)	$W^U$ (lb)	$\left(\frac{D_c(t_r)}{D_c}\right)^3$	$W^U(t_r)$ (lb)
a	0.08	0.0127	2.50	0.76	3.26	3.26	100	0.45	45
b	.12	.0191	2.50	.76	3.26	3.12	130	.45	59

The generalized results apply for reactors operating in the thermal temperature range of  $1400^\circ$  to  $1500^\circ$  F; for lower temperatures, investments are slightly lower than indicated by figure 7.

#### Typical Neutron Flux and Heat-Generation Distributions

Two-group neutron flux and heat-generation distributions have been determined for reactors I and III and are presented herein as representative of NaOH-cooled and moderated reactors. The distributions are presented as a function of cylinder radius for an equivalent spherical reactor as an indication of the distributions for the cylindrical geometry.

Neutron flux distributions. - The fast and thermal neutron flux distributions are shown in figure 8 for the 6-inch reflector thickness

and for a value of atom ratio  $R$  of 100 (indicated in figure 4 to be near the minimum investment point). For convenience, the flux values shown correspond to reactor total power output of 300,000 kilowatts; inasmuch as fluxes are directly proportional to power, they may be adjusted for power outputs other than 300,000 kilowatts. Flux levels for the same total power output are higher for reactor III than for reactor I principally because of the smaller core size possible with reactor III.

Because of the smaller absorption in reactor III, thermal neutrons resulting from slowing down in the reflector can penetrate farther into the core of reactor III than reactor I. Hence, the effectiveness of the reflector toward flattening the thermal flux in the core is greater in reactor III than I; for example, the ratio of minimum to maximum thermal flux in the core is 0.65 and 0.43 for reactors III and I, respectively.

The ratio of fast to thermal neutron flux is about 9 for reactor I and about 7 for reactor III. These ratios will decrease as reactor size and corresponding investment are increased and less dependence upon fast fissions is required.

Heat-generation distributions. - Radial heat-generation distributions are shown in figure 9 for various values of reflector thickness and for the value of  $R$  equal to 100. Figure 9 is a plot of the ratio of local specific heat release to average specific heat release against reactor core radius expressed as a fraction of total core radius.

The distributions demonstrate the degree to which reactors with NaOH reflectors may be expected to approach uniform heat generation with uniform distribution of uranium. The effect of reflector thickness saturates rapidly with little change in distribution above thicknesses of 6 inches.

Larger variations in local heat release with radius are to be expected of reactors containing appreciable concentrations of absorptive structure, inasmuch as these reactors depend in greater measure upon the fast flux to provide fissions than reactors with little absorptive structure. In addition, as previously mentioned, neutrons which enter the core after being slowed down in the reflector do not penetrate as far into the core for reactor I as they do for reactor III, thus contributing to further nonuniformity in the power-generation distribution.

These two points are illustrated in figure 10 in which the fraction of total local fissions produced thermally is presented as a function of core radius for reactors I and III for various reflector thicknesses. It may be seen that reactor I has about 6 percent fewer thermal fissions than reactor III throughout the core. In addition, the high concentration of thermal fissions at the core-reflector interface falls off more rapidly

for reactor I than for reactor III. It is noted that these reactors can be classified as intermediate reactors in that about 40 percent of total fissions are produced in the fast neutron group.

The heat-generation distribution over the reactor core volume can be varied by nonuniform distribution of fissionable material. Reference 16, which presents fissionable-material distributions corresponding to uniform heat generation for a representative thermal reactor assembly with various reflector thicknesses, indicates that appreciable improvement in power-generation distribution can be achieved in a well reflected reactor by redistribution of the fissionable material with only a small additional investment of fissionable material (of the order of 10 to 15 percent for the assemblies of reference 16). Although the results of reference 16 are for thermal reactors in which the fissionable material was redistributed to give uniform heat generation, the same general conclusions should apply for the intermediate reactors presently under consideration for which the fissionable material may be redistributed to attain uniform fuel-element temperature throughout the reactor core volume.

2525

#### Static Stability Characteristics and Excess Uranium Requirements

The temperature coefficient of reactivity and excess uranium requirements have been computed for reactors I and III. Two representative examples of each reactor have been considered (an intermediate reactor of small core size and a more thermal reactor of relatively large core size) in order to illustrate both the effect of structure and the effect of neutron leakage on reactor stability. Reactors reflected with a 6-inch thickness of NaOH have been considered for both cases.

The radial distribution of adjoint functions  $\varphi_f^+$  and  $\varphi_{th}^+$  relative to the value of  $\varphi_{th}^+$  at the reactor axis, for the smaller hot, unpoisoned reactors I and III with an atom ratio  $R$  of 100, are presented in figure 11. These adjoint functions, computed in accordance with the methods described in appendix D, are used in conjunction with the actual neutron flux distributions to provide weighting factors which evaluate the relative importance of small local changes or perturbations of the reactor constants at any reactor geometrical position.

For example, the effect on pile reactivity of a small change in thermal absorption cross section  $\Sigma_{A,th}$  at a particular position of the reactor core is proportional to the product of the thermal flux and the thermal adjoint function at that position. The over-all effect on reactivity of small changes in  $\Sigma_{A,th}$  over the entire reactor core is evaluated by the integrated effect over the entire core volume as shown in appendix D.

*2525*

Temperature coefficient of reactivity. - Temperature coefficients of reactivity have been computed for both poisoned and unpoisoned reactors operating at 1450° F and a power of 300,000 kilowatts. Excess uranium requirements have been estimated for these reactors on the assumption that the reactors were predominantly thermal. The poisoned condition considers the equilibrium xenon concentration and concentrations of 24-hour accumulation of samarium and fission products for operation at a constant power of 300,000 kilowatts; these concentrations are listed on the following table for the reactors considered:

Reactor	H/U atom ratio, R	Core diameter (ft)	Average thermal flux $\Phi_{th}$	$N_{Xe}$ (atoms/cc core)	$N_{Sa}$ (atoms/cc core)	$N_{fiss. prod.}$ (atoms/cc core)
I	100	2.26	$4.77 \times 10^{14}$	$2.85 \times 10^{15}$	$7.75 \times 10^{15}$	$3.14 \times 10^{18}$
I	200	5.34	.85	.11	.88	.23
III	100	1.52	16.50	2.81	7.73	10.0
III	400	3.10	9.70	.55	2.00	1.17

Reactors are reflected by 6-inch thickness of NaOH.

Individual temperature coefficients of reactivity associated with changes with temperature of the two-group parameters for each of the four reactors are listed in table IV. Derivatives of each parameter with temperature were obtained numerically from the calculated variation of the parameter with temperature and satisfactorily represent actual derivatives for the temperature range from about 1200° to 1700° F. Temperature coefficients of reactivity  $dp/dT$  were computed by the relations given in appendix D.

In the calculation of  $dp/dT$  for reactor III which does not contain fuel-element structure and would therefore physically correspond to the homogeneous reactor, it has been assumed that the uranium concentrations remain fixed and that only the cross section varies with temperature; results for reactors I and III given in the table are then directly comparable. Of course, the reduction in uranium concentration accompanying the expansion of NaOH in a homogeneous reactor would produce a substantially more negative temperature coefficient of reactivity for reactor III.

From table IV it may be noted that the combined contribution to the temperature coefficient of  $\Sigma_{A,th}$  (without poison),  $K_{th}$ ,  $\Sigma_{A,th}$ ,  $\Sigma_{A,f}$ , and  $K_f \Sigma_{A,f}$ , that is, of the fission and absorption processes, is relatively small. The effect of the poisons (given by difference in contributions of  $\Sigma_{A,th}$  with and without poison) is slightly positive.

The combined contributions of  $\lambda_{TR,th}$ ,  $\lambda_{TR,f}$ , and  $\Sigma_{s,f}$ , that is, of the scattering and slowing-down processes, give a relatively large negative temperature coefficient which is associated mainly with the decrease in density of moderator with increase in temperature. As a result of this large negative contribution, the over-all temperature coefficients of the reactors considered are negative. The magnitude of the negative temperature coefficient increases as the size of the reactor decreases.

Net values of the temperature coefficient of reactivity  $d\rho/dT$  vary from about -0.00006 for the small-sized reactors to about -0.00002 for the large reactors. A temperature coefficient of reactivity of about -0.00006 per  $^{\circ}\text{F}$  results in a change in reactivity of -0.6 percent for a  $100^{\circ}\text{ F}$  temperature rise; this reactivity is of the same order of magnitude as that associated with the delayed-fission neutrons and so indicates the negative coefficient to be significant from the point of view of steady-state reactor self-control.

Excess uranium requirements. - The excess uranium requirement  $\Delta W^U$  for the poisoned critical reactor over the investment required for the unpoisoned critical reactor,  $W^U$ , is also listed in table IV. It may be seen that the excess uranium requirement necessary to maintain criticality for these reactors after 24-hour operation at a power of 300,000 kilowatts increases as the size of the reactor producing this power decreases. The excess uranium requirement appears to be less than 10 pounds for all the reactors herein considered.

#### Reactor Heat-Transfer Characteristics

It is recalled that the reactor heat-transfer characteristics presented are independent of any airplane considerations. The results are presented per kilowatt of total reactor heat release and are related to the airplane only when the power requirements for a particular flight condition are established.

Figure 12 presents plots of the difference between maximum fuel-element temperature and average NaOH coolant temperature per kilowatt of total reactor heat release,  $\frac{T_w,ex - T_c,av}{H}$ , against coolant velocity.

Each plot is for a given core diameter (2, 2.5, or 3 ft) and concentration of structural material (6 or 12 percent by volume) for fuel-element plate thicknesses of 0.012, 0.016, and 0.020 inch. Heat generation is assumed to be uniform over the reactor core for the 0.016- and 0.020-inch plate thicknesses; for the 0.012-inch plate thickness, both cases of uniform heat generation and of uniform fuel-element wall temperature are presented. Also included in each plot is the difference between the exit and average NaOH temperature. The effects of pertinent

variables on the difference between maximum fuel-element temperature and exit coolant temperature are directly obtainable from figure 12.

The following tabulation of results, obtained from figure 12 for a reactor with total heat release of 300,000 kilowatts, indicates the effects on  $T_{w,ex} - T_{c,av}$  of representative values of the heat-transfer variables.

$D_c$ (ft)	$V_c$ (ft/sec)	$f_s$	$t_p$ (in.)	Reactor operation	$T_{w,ex} - T_{c,av}$ (°F)
2.0	15	0.06	0.012	UHG <sup>a</sup>	390
2.5	15	.06	.012	UHG	210
3.0	15	.06	.012	UHG	125
2.5	30	.06	.012	UHG	125
2.5	15	.12	.012	UHG	80
2.5	15	.06	.020	UHG	365
2.5	15	.06	.012	UWT <sup>b</sup>	165

<sup>a</sup>Uniform heat generation

<sup>b</sup>Uniform wall temperature

#### Airplane and Turbojet Cycle Characteristics

Flight condition requirements. - Figures 13 and 14 present plots of reactor heat release  $H$ , and airplane gross weight  $W_g$  (expressed in ratio to shield, reactor, pay-load, and auxiliary weight  $W_K$ ) against effective wall temperature of the air heat exchanger  $T_{w,eff}$  for flight at 30,000- and 50,000-foot altitudes at Mach numbers of 0.9 and 1.5. The optimized turbojet cycle conditions determined in reference 14 for each of these flight conditions were used in the construction of these plots.

Figure 13 shows that the effect of flight speed on reactor heat release is much greater than the effect of altitude, chiefly because of the greatly reduced airplane lift-drag ratios (and hence increased power requirements) encountered at supersonic speeds. For  $T_{w,eff}$  about 1700° F, heat releases required for supersonic flight are of the order of three times greater than for subsonic flight; for  $T_{w,eff}$  about 1100° F, the heat-release requirements are of the order of five times greater. For the range of values of  $T_{w,eff}$  plotted in figure 13, heat releases for subsonic flight are fairly insensitive to variation in  $T_{w,eff}$ ; for supersonic flight, heat releases are quite sensitive to  $T_{w,eff}$ , particularly in the range below 1200° F.

Figure 14 shows that reduction of altitude from 50,000 feet to 30,000 feet for the 1.5 Mach number significantly reduces gross weight requirements to the point where the gross weights are comparable with subsonic values.

Maximum reactor fuel-element temperature. - The reactor heat transfer and the turbojet cycle characteristics have been combined to establish the magnitude of maximum reactor temperatures required for the four flight conditions considered.

Maximum fuel-element temperatures are plotted in figures 15 and 16 against reactor heat releases required for the four flight conditions considered, for reactor operation at uniform heat generation and uniform wall temperature, and for the following conditions:

Figure 15 is for  $W_K$  of 100,000 pounds; figure 16 is for  $W_K$  of 150,000 pounds. Four separate plots are included in each figure, one for each of the four flight conditions.

The NaOH coolant temperature leaving the reactor is included in the figures as an indication of the limit to which the maximum fuel-element temperature may be reduced. It is recalled that an assumed temperature difference of 100° F between the average NaOH temperature in the reactor and the effective wall temperature in the air heat exchanger has been incorporated in the data of figures 15 and 16.

For a given reactor configuration and allowable maximum fuel-element temperature, figures 15 and 16 provide a value of reactor heat release required for any of the four flight conditions considered. Corresponding values of gross airplane weight may be obtained from figures 13 and 14 with  $T_w$ ,<sub>eff</sub> as the linking variable.

Figures 15 and 16 indicate the following general results for the two values of  $W_k$  considered:

(a) At subsonic flight (Mach number 0.9), maximum fuel-element temperature can be maintained at  $1200^{\circ}$  F and lower for reactor core diameters of 2 feet and volume concentrations of fuel-element material of 6 percent with reasonable values of reactor heat release and airplane gross weight. At  $1200^{\circ}$  F, these values are tabulated as follows:

$W_K$ (lb)	Altitude (ft)	H (kw)	$W_g$ (lb)
100,000	50,000	68,000	198,000
100,000	30,000	59,000	160,000
150,000	50,000	106,000	305,000
150,000	30,000	90,000	242,000

2525

Variation in reactor core diameter and volume concentration of fuel-element material has relatively little effect on maximum fuel-element temperature for a given reactor heat release. A maximum fuel-element temperature of about  $1100^{\circ}$  F can be attained by an increase in reactor core diameter to 2.5 feet or by an increase in volume of fuel-element material to 12 percent with operation at the following conditions:

$W_K$ (lb)	Altitude (ft)	H (kw)	$W_g$ (lb)
100,000	50,000	72,000	205,000
100,000	30,000	61,000	163,000
150,000	50,000	110,000	310,000
150,000	30,000	93,000	246,000

For the subsonic flight conditions it is noted that the increase in reactor heat release and airplane gross weight, resulting from a decrease in maximum fuel-element temperature from  $1200^{\circ}$  to  $1100^{\circ}$  F, is small. There appears to be a small advantage in reactor operation at uniform element temperature over operation at uniform power generation.

(b) At supersonic flight (Mach number 1.5), maximum fuel-element temperatures must be of the order of  $1500^{\circ}$  to  $1700^{\circ}$  F for a reactor core diameter of 2 feet and volume concentration of fuel-element material of 6 percent. Increase in reactor core diameter to 2.5 feet and volume of fuel-element material to 12 percent lowers fuel-element temperature to the  $1200^{\circ}$  to  $1300^{\circ}$  F level. For these conditions and a maximum fuel-element temperature of  $1200^{\circ}$  F, the following tabulation is made:

$W_K$ (lb)	Altitude (ft)	H (kw)	$W_g$ (lb)
100,000	50,000	340,000	295,000
100,000	30,000	260,000	180,000
150,000	50,000	590,000	500,000
150,000	30,000	410,000	275,000

Reference to figures 13 and 14 indicates that operation at the lower values of air heat-exchanger effective wall temperature seriously penalizes the airplane gross weight and required heat release for the supersonic 50,000-foot-altitude condition, but that flight at a Mach number of 1.5 at an altitude of 30,000 feet requires a larger heat release but a relatively smaller gross weight which is comparable with subsonic requirements.

Summary of airplane conditions with low-temperature turbojet cycle. - For convenience in evaluation of the airplane engine and reactor requirements for the four flight conditions considered, a summary is presented in table V of some representative results obtained in the airplane cycle performance, heat transfer, and reactor criticality study.

The turbojet operating conditions and airplane component weights listed are based on engine operation at an air heat-exchanger effective wall temperature of  $1000^{\circ}$  F at all flight conditions. A difference of  $100^{\circ}$  F between the average NaOH reactor coolant temperature and the air heat-exchanger effective wall temperature is maintained.

The actual total engine air flow to the turbojet engines at each flight condition is listed; in addition, the total engine air flow corrected to static sea-level conditions is included. (The corrected air flow is used to specify the air-handling capacity of a turbojet engine.) From designs of existing engines, it appears that a corrected air flow of about 300 pounds per second is obtainable with a turbojet engine approximately 4 feet in diameter. The corrected total engine air flow therefore serves as a measure of the number of turbojet engines required to maintain a given flight condition; these values are also listed in table V.

Six and nine engines of the size specified are required to maintain flight at 30,000 feet altitude and Mach number 1.5 for respective values of  $W_K$  of 100,000 and 150,000 pounds. This compares reasonably well with the numbers of engines required for both subsonic conditions. Supersonic flight at 50,000 feet altitude, however, requires on this basis 20 engines for a  $W_K$  of 100,000 pounds, and 29 engines for a  $W_K$  of 150,000 pounds. The large number of engines required for this flight condition may impair aerodynamic characteristics and reduce obtainable lift-drag ratios below the assumed value of 6.5.

For supersonic flight at 50,000 feet altitude, the air heat-exchanger effective wall temperature would have to be increased to about  $1600^{\circ}$  F, in order to reduce the required air flows to values comparable with the other flight conditions.

Two reactor geometries of diameters 2.0 and 2.5 feet have been selected for operation at each flight condition. Both configurations provide for relatively low maximum fuel-element temperatures consistent with the attainment of reasonable airplane gross weights and reactor

heat releases. The uranium investments required for these reactors are below 50 pounds.

#### SUMMARY OF RESULTS

The effects of reactor variables on criticality and maximum reactor fuel-element temperatures for sodium-hydroxide-cooled, moderated, and reflected reactors of length-diameter ratio 1 are presented for subsonic and supersonic propulsion of nuclear-powered aircraft. The following results, based on turbojet engine cycle operating conditions optimized to give minimum airplane gross weight, were obtained from the study for two values of weight of shield plus reactor plus pay-load plus auxiliaries (designated as  $W_K$ ) representative of the divided-type shadow shield and the unit bulk shield, respectively:

1. Flight at a Mach number of 0.9 at altitudes of 30,000 and 50,000 feet for values of  $W_K$  of 100,000 and 150,000 pounds may be maintained with maximum reactor fuel-element temperatures of the order of  $1100^\circ$  to  $1200^\circ$  F with a reactor core diameter of 2 feet.
2. An airplane gross weight of about 200,000 pounds and reactor heat release of about 70,000 kilowatts are required for subsonic flight for  $W_K$  of 100,000 pounds. Gross weight and reactor heat release are proportionately increased for a value of  $W_K$  of 150,000 pounds.
3. Flight at a Mach number of 1.5 at an altitude of 30,000 feet for both values of  $W_K$  may be maintained with maximum reactor fuel-element temperatures of the order of  $1200^\circ$  to  $1300^\circ$  F with a reactor core diameter of 2 feet. At an altitude of 50,000 feet and a Mach number of 1.5, similar maximum fuel-element temperatures may be maintained with a reactor core diameter of 2.5 feet.
4. At 30,000 feet altitude, airplane gross weight for supersonic flight is comparable with gross weight requirements for subsonic flight (about 180,000 pounds for  $W_K$  of 100,000 pounds); reactor heat releases required, however, are about four times greater than for the subsonic case (270,000 kilowatts for  $W_K$  of 100,000 pounds). At 50,000 feet altitude, airplane gross weights and reactor heat releases required for supersonic flight are about 300,000 pounds and 350,000 kilowatts respectively, for  $W_K$  of 100,000 pounds. Gross weight and heat release are proportionately increased for  $W_K$  of 150,000 pounds.
5. Enriched uranium investments for the hot unpoisoned reflected reactor, containing sufficient high-nickel-alloy fuel elements to provide appropriate heat-transfer surface for the aforementioned reactor and airplane flight conditions, are of the order of 35 and 50 pounds for core diameters of 2.0 and 2.5 feet, respectively. As fuel-element structural material in the reactor is reduced to zero concentration, the uranium investments approach 15 and 20 pounds for the 2.0- and 2.5-foot core diameters, respectively. The excess uranium required to

counteract burnup and the poisoning effects of equilibrium xenon, samarium, and other fission products, resulting from reactor operation for 24 hours at 300,000 kilowatts, is estimated to be less than 10 pounds. At this poisoned condition, the temperature coefficient of reactivity for reactors with high-nickel-alloy fuel elements was calculated to be negative and of the order of -0.00006 per °F.

Lewis Flight Propulsion Laboratory  
National Advisory Committee for Aeronautics  
Cleveland, Ohio, July 28, 1952

2525

## APPENDIX A - SYMBOLS

A	reactor coolant flow area
$c_p$	coolant specific heat
D	neutron diffusion length
$D_c$	reactor core diameter
$\Delta D_c$	reduction in reactor diameter due to reflector
$D_e$	equivalent diameter of coolant flow passage
E	neutron energy
$F_n$	airplane net thrust
$f_s$	volume fraction of structural and fuel-element material in reactor core
H	reactor heat release
h	reactor heat-transfer coefficient
K	neutron multiplication constant
$k_s$	thermal conductivity of fuel-element material
$k$	coolant thermal conductivity
$L_c$	reactor core length
$L_f^2$	mean square slowing-down distance for fast neutrons
$L_{th}^2$	mean square diffusion distance for thermal neutrons
L/D	airplane lift-drag ratio
$M(v)$	Maxwellian neutron density (per unit speed range)
N	reactor atom density
$P_{th}$	resonance escape probability
q	neutron slowing-down density
R	ratio of hydrogen to uranium 235
$R_c$	reactor core radius

r	reactor radius
S	reactor heat-transfer surface area
sp	fuel-element plate spacing
T	temperature
$T_{c,av}$	average reactor coolant temperature
$T_{c,en}$	coolant temperature entering reactor
$T_{c,ex}$	coolant temperature leaving reactor
$T_{w,eff}$	air heat-exchanger effective wall temperature
$T_{w,ex}$	maximum fuel-element temperature
$T_{w,ex}^0$	maximum fuel-element surface temperature
$t_p$	plate-type fuel-element sandwich thickness
$t_r$	reactor reflector thickness
$u = \log_e \frac{10^7}{E}$	logarithmic neutron energy
v	coolant velocity
v	neutron velocity
$W_g$	airplane gross weight
$W_K$	shield, reactor, pay-load, and auxiliary equipment weight
$W_s$	airplane structural weight
$W^U$	enriched uranium investment
$\Delta W^U$	excess uranium requirement
$w_a$	turbojet-engine air flow
$\delta$	extrapolation distance
$\lambda_{TR}$	macroscopic transport mean free path
$\mu$	coolant viscosity

2525

$v$	neutrons produced per fission
$\xi$	average logarithmic energy loss per collision
$\rho$	coolant density
$\frac{dp}{dT}$	temperature coefficient of reactivity
$\Sigma_A$	macroscopic absorption cross section
$\Sigma_{A,th}^s$	macroscopic absorption cross section of structural material
$\Sigma_F$	macroscopic fission cross section
$\Sigma_S$	macroscopic scattering cross section
$\Sigma_T$	macroscopic total cross section
$\sigma_S$	microscopic scattering cross section
$\varphi$	neutron flux
$\varphi^+$	adjoint function

## Subscripts:

0	reactor core
1	reactor reflector
m	moderator
th	thermal neutron group
f	fast neutron group

## APPENDIX B - TWO-GROUP DIFFUSION THEORY

Two-group two-zone diffusion equations. - The neutrons are separated into two groups: a fast group consisting of all neutrons from fission energies to thermal energy, and a thermal group consisting of all slowed-down neutrons in statistical equilibrium with the temperature of their surroundings.

For the fast group, terms representing leakage, absorption, slowing out, and production of neutrons in the reactor core are given by

$$\text{Leakage: } -\frac{\lambda_{TR,f,0}}{3} \Delta \Psi_{f,0}$$

$$\text{Absorption: } \Sigma_{A,f,0} \Psi_{f,0}$$

$$\text{Slowing out: } \Sigma_{S,f,0} \Psi_{f,0}$$

$$\text{Production: } \Sigma_{F,f,0} v \Psi_{f,0} + \Sigma_{F,th,0} v \Psi_{th,0}$$

For the thermal group, terms representing leakage, absorption, and production of neutrons in the reactor core are given by

$$\text{Leakage: } -\frac{\lambda_{TR,th,0}}{3} \Delta \Psi_{th,0}$$

$$\text{Absorption: } \Sigma_{A,th,0} \Psi_{th,0}$$

$$\text{Production: } \Sigma_{S,f,0} \Psi_{f,0}$$

For the reflector, terms representing leakage, absorption, and slowing out of the fast group are given by

$$\text{Leakage: } -\frac{\lambda_{TR,f,1}}{3} \Delta \Psi_{f,1}$$

$$\text{Absorption: } \Sigma_{A,f,1} \Psi_{f,1}$$

$$\text{Slowing out: } \Sigma_{S,f,1} \Psi_{f,1}$$

Terms representing leakage, absorption, and production of neutrons for the thermal group of the reflector are given by

$$\text{Leakage: } -\frac{\lambda_{TR,th,1}}{3} \Delta \Psi_{th,1}$$

$$\text{Absorption: } \Sigma_{A,th,1} \Psi_{th,1}$$

$$\text{Production: } \Sigma_{S,f,1} \Psi_{f,1}$$

The macroscopic cross sections and mean free paths appearing in the foregoing terms must be appropriately averaged over the energy range constituting the pertinent neutron group so that the various terms represent the correct distribution of neutron processes occurring within the reactor.

For each group and reactor zone, expressions for the conservation of neutrons may be written

$$- \frac{\lambda_{TR,f,0}}{3} \Delta \varphi_{f,0} + (\Sigma_{A,f,0} + \Sigma_{S,f,0}) \varphi_{f,0} - \Sigma_{F,f,0} v \varphi_{f,0} - \Sigma_{F,th,0} v \varphi_{th,0} = 0 \quad (B1)$$

$$- \frac{\lambda_{TR,th,0}}{3} \Delta \varphi_{th,0} + \Sigma_{A,th,0} \varphi_{th,0} - \Sigma_{S,f,0} \varphi_{f,0} = 0 \quad (B2)$$

$$- \frac{\lambda_{TR,f,1}}{3} \Delta \varphi_{f,1} + (\Sigma_{A,f,1} + \Sigma_{S,f,1}) \varphi_{f,1} = 0 \quad (B3)$$

$$- \frac{\lambda_{TR,th,1}}{3} \Delta \varphi_{th,1} + \Sigma_{A,th,1} \varphi_{th,1} - \Sigma_{S,f,1} \varphi_{f,1} = 0 \quad (B4)$$

These equations may be rearranged as follows:

$$\Delta \varphi_{f,0} - \frac{3(\Sigma_{A,f,0} + \Sigma_{S,f,0})}{\lambda_{TR,f,0}} \varphi_{f,0} + \frac{3}{\lambda_{TR,f,0}} \frac{\Sigma_{F,f,0} v}{\Sigma_{A,f,0}} \Sigma_{A,f,0} \varphi_{f,0} + \frac{3}{\lambda_{TR,th,0}} \frac{\lambda_{TR,th,0}}{\lambda_{TR,f,0}} \frac{\Sigma_{F,th,0} v}{\Sigma_{A,th,0}} \Sigma_{A,th,0} \varphi_{th,0} = 0 \quad (B5)$$

$$\Delta \varphi_{th,0} - \frac{3\Sigma_{A,th,0}}{\lambda_{TR,th,0}} \varphi_{th,0} + \frac{3\Sigma_{S,f,0}}{\lambda_{TR,f,0}} \frac{\lambda_{TR,f,0}}{\lambda_{TR,th,0}} \varphi_{f,0} = 0 \quad (B6)$$

$$\Delta \varphi_{f,1} - \frac{3(\Sigma_{A,f,1} + \Sigma_{S,f,1})}{\lambda_{TR,f,1}} \varphi_{f,1} = 0 \quad (B7)$$

$$\Delta \varphi_{th,1} - \frac{3\Sigma_{A,th,1}}{\lambda_{TR,th,1}} \varphi_{th,1} + \frac{3\Sigma_{S,f,1}}{\lambda_{TR,f,1}} \frac{\lambda_{TR,f,1}}{\lambda_{TR,th,1}} \varphi_{f,1} = 0 \quad (B8)$$

The mean-square slowing-down length  $L_{f,0,1}^2$  and mean-square thermal diffusion length  $L_{th,0,1}^2$  are defined as

$$L_{f,0,1}^2 = \frac{\lambda_{TR,f,0,1}}{3(\Sigma_{A,f,0,1} + \Sigma_{S,f,0,1})}$$

$$L_{th,0,1}^2 = \frac{\lambda_{TR,th,0,1}}{3\Sigma_{A,th,0,1}}$$

Inasmuch as the macroscopic cross sections are the effective averages over the pertinent energy group, the resonance escape probability may be suitably approximated in terms of these effective values.

$$p_{th,0,1} = \frac{\Sigma_{S,f,0,1}}{(\Sigma_{A,f,0,1} + \Sigma_{S,f,0,1})}$$

It follows then that

$$\frac{\lambda_{TR,f,0,1}}{3\Sigma_{S,f,0,1}} = \left( \frac{\Sigma_{A,f,0,1} + \Sigma_{S,f,0,1}}{\Sigma_{S,f,0,1}} \right) L^2_{f,0,1} = \frac{L^2_{f,0,1}}{p_{th,0,1}}$$

$$\frac{\lambda_{TR,f,0,1}}{3\Sigma_{A,f,0,1}} = \left( \frac{\Sigma_{A,f,0,1} + \Sigma_{S,f,0,1}}{\Sigma_{A,f,0,1}} \right) L^2_{f,0,1} = \frac{L^2_{f,0,1}}{(1-p_{th,0,1})}$$

The multiplication constants  $K_f$  and  $K_{th}$  representing, respectively, the number of neutrons born per neutron absorbed in each energy group are defined as

$$K_f = \frac{\Sigma_{F,f,0}}{\Sigma_{A,f,0}} v$$

$$K_{th} = \frac{\Sigma_{F,th,0}}{\Sigma_{A,th,0}} v$$

With these definitions, the two-group equations may be rewritten. For the core,

$$\Delta \varphi_{f,0} - \left[ \frac{1-K_f(1-p_{th,0})}{L^2_{f,0}} \right] \varphi_{f,0} + \frac{\lambda_{TR,th,0}}{\lambda_{TR,f,0}} \frac{K_{th}}{L^2_{th,0}} \varphi_{th,0} = 0 \quad (B9)$$

$$\Delta \varphi_{th,0} - \frac{1}{L^2_{th,0}} \varphi_{th,0} + \frac{\lambda_{TR,f,0}}{\lambda_{TR,th,0}} \frac{p_{th,0}}{L^2_{f,0}} \varphi_{f,0} = 0 \quad (B10)$$

For the reflector

$$\Delta \varphi_{f,1} - \frac{1}{L_{f,1}^2} \varphi_{f,1} = 0 \quad (B11)$$

$$\Delta \varphi_{th,1} - \frac{1}{L_{th,1}^2} \varphi_{th,1} + \frac{\lambda_{TR,f,1}}{\lambda_{TR,th,1}} \frac{p_{th,1}}{L_{f,1}^2} \varphi_{f,1} = 0 \quad (B12)$$

2525

Boundary conditions and solutions. - The preceding simultaneous linear differential equations are solved subject to the following boundary conditions for the case of spherical geometry.

The continuity of neutron current at the core-reflector interface requires that

$$\left. \begin{aligned} -\frac{\lambda_{TR,f,0}}{3} \nabla \varphi_{f,0} \end{aligned} \right|_{r=R_c} = \left. \begin{aligned} -\frac{\lambda_{TR,f,1}}{3} \nabla \varphi_{f,1} \end{aligned} \right|_{r=R_c} \quad \left. \begin{aligned} -\frac{\lambda_{TR,th,0}}{3} \nabla \varphi_{th,0} \end{aligned} \right|_{r=R_c} = \left. \begin{aligned} -\frac{\lambda_{TR,th,1}}{3} \nabla \varphi_{th,1} \end{aligned} \right|_{r=R_c} \quad \left. \begin{aligned} \end{aligned} \right\} \quad (B13)$$

The continuity of neutron flux at the interface also requires that

$$\left. \begin{aligned} \varphi_{f,0} \end{aligned} \right|_{r=R_c} = \left. \begin{aligned} \varphi_{f,1} \end{aligned} \right|_{r=R_c} \quad \left. \begin{aligned} \varphi_{th,0} \end{aligned} \right|_{r=R_c} = \left. \begin{aligned} \varphi_{th,1} \end{aligned} \right|_{r=R_c} \quad \left. \begin{aligned} \end{aligned} \right\} \quad (B14)$$

At the outer face of the reflector, the neutron fluxes must go to zero at the extrapolated boundary; it is assumed that the extrapolation distance is the same for both fast and thermal neutrons and small in comparison with the reflector thickness so that

$$\left. \begin{aligned} \varphi_{f,1} \end{aligned} \right|_{r=R_c+t_r} = 0 \quad \left. \begin{aligned} \varphi_{th,1} \end{aligned} \right|_{r=R_c+t_r} = 0 \quad \left. \begin{aligned} \end{aligned} \right\} \quad (B15)$$

The neutron fluxes must be finite everywhere in the reactor, that is

$$\left. \begin{array}{l} \Psi_f \\ \Psi_{th} \end{array} \right]_{\text{all } r < \infty} \quad \left. \begin{array}{l} \\ \end{array} \right\} \quad (B16)$$

The general solutions of the pairs of simultaneous equations (9) to (12) are obtained by letting  $\Delta\Psi = \alpha^2\Psi$  where  $\alpha^2$  is the same constant for the fast and thermal fluxes in each zone but differs for the core and reflector zones;  $\alpha^2$  is designated as  $\alpha_0^2$  for the core and as  $\alpha_1^2$  for the reflector. Introduction of  $\Delta\Psi_{0,1} = \alpha_{0,1}^2\Psi_{0,1}$  in equations (9) to (12) yields quadratic expressions for  $\alpha_0^2$  and  $\alpha_1^2$  in terms of the core and reflector compositions, respectively. The general solution for the fast or thermal flux in each zone is then a linear combination of the general solutions of  $\Delta\Psi = \alpha^2\Psi$  corresponding to the two roots of the quadratic appropriate for each zone.

2525

Application of the foregoing boundary conditions to the general solutions for the fast and thermal flux in each zone leads to four homogeneous linear equations involving four arbitrary constants and the unknown critical radius of the reactor core and thickness of the reflector. The vanishing of the determinant of coefficients of these four equations for an assigned thickness of reflector is the condition for the evaluation of the critical radius of the core.

With the critical dimensions of the reactor known, three of the arbitrary constants are solved for in terms of the fourth. The flux distributions in both the core and reflector are therefore determined except for an arbitrary multiplicative constant. Detailed mechanics of the two-group method are presented in references 17 and 18.

The reflected reactor sizes calculated for spherical geometry are translated to cylindrical geometry in the following manner:

(a) For the unreflected reactor, the critical sizes are determined by the relations

$$\alpha_0^2 = \frac{\pi^2}{(R'_c + \delta)^2} \quad \text{for spherical geometry}$$

$$\alpha_0^2 = \frac{\pi^2}{(H_c + 2\delta)^2} + \frac{2.405^2}{(R_c + \delta)^2} \quad \text{for cylindrical geometry}$$

where the buckling constant  $\alpha_0^2$  is a function only of the composition of the unreflected reactor and hence is independent of the geometry of the system. ( $R_c$  is here the cylinder radius,  $R'_c$  the sphere radius, and  $\delta$  the extrapolation distance at which the flux becomes zero.) Hence, for the same reactor composition,

$$\frac{\pi^2}{(R'_c + \delta)^2} = \frac{\pi^2}{(H_c + 2\delta)^2} + \frac{2.405^2}{(R_c + \delta)^2}$$

or, if the cylindrical reactor is of length-diameter ratio equal to unity  $H_c = 2R_c$ ,

$$R_c + \delta = 0.9144 (R'_c + \delta)$$

For  $\delta \ll R_c, R'_c$

$$\frac{R_c}{R'_c} \approx 0.9144$$

(b) For the reflected reactor, the assumption is made that the reflector savings (difference in core radii for unreflected and reflected reactors) is the same for both the spherical and cylindrical geometries. Hence the reflector savings calculated for any given core and reflector thickness for the spherical geometry can be directly applied to the unreflected cylindrical critical dimensions to obtain the reflected cylindrical critical dimensions.

Effect of voids on criticality of bare reactor. - The introduction of uniformly distributed void space in a bare reactor reduces the densities of all constituents in the reactor by the factor  $(1-f_v)$  where  $f_v$  is here the fraction of void volume. Hence, all macroscopic cross sections are reduced by the factor  $(1-f_v)$ . The relation between  $\alpha_0^2$  and the reactor nuclear constants (see references 17 and 18) shows that  $\alpha_0^2$  is then reduced by the factor  $(1-f_v)^2$  for the same relative core composition. Hence, the critical dimensions of the bare reactor are increased by the

factor  $\frac{1}{(1-f_v)}$ , that is

$$\frac{D \left[ \text{with void} \right]}{D \left[ \text{no void} \right]} = \frac{1}{(1-f_v)}$$

For the same relative core composition, the uranium investment is directly proportional to its reactor concentration and to the reactor volume; that is,

$$\frac{W^U \left[ \text{with void} \right]}{W^U \left[ \text{no void} \right]} = (1-f_v) \frac{D^3 \left[ \text{with void} \right]}{D^3 \left[ \text{no void} \right]} = \frac{1}{(1-f_v)^2}$$

Effect of voids on criticality of reflected reactor. - The assumption is made that the reflector savings are unaffected by introduction of small amounts of void volume in the core of a reflected reactor.

## APPENDIX C - EVALUATION OF TWO-GROUP THEORY CONSTANTS

The constants required for solution of the two-group equations are as follows:

$L_f^2$	mean-square slowing-down length
$L_{th}^2$	mean-square thermal diffusion length
$\lambda_{TR,f}$	fast-transport mean free path
$\lambda_{TR,th}$	thermal-transport mean free path
$p_{th}$	resonance escape probability
$K_f$	fast multiplication constant
$K_{th}$	thermal multiplication constant

These constants are separately evaluated for each core and reflector composition. Multiplication constants are, of course, zero for the reflector.

The fast parameters were averaged over the energy spectrum of neutrons born during fission. The thermal fission neutron spectrum was taken from reference 5 and normalized to unity over an energy range extending from 25,000 ev to 10 Mev.

Total cross sections for Na, O, H, Ni, and Fe as a function of neutron energy were taken from reference 8. Resonances for these nuclei occur only at 3000 ev and above; for these energies the neutron scattering width is very much larger than the neutron absorption width so that these resonances have been taken as substantially scattering. The values used for total cross section for H were those obtained from measurements in  $H_2O$ .

Thermal absorption cross sections were taken from reference 19; the pile oscillator values were used wherever available. The variation of absorption cross section with neutron energy was assumed to follow the  $1/v$  law.

Fission, absorption, and scattering cross sections for K-25 end product uranium mixture (91.5 percent  $U^{235}$ , 1.5 percent  $U^{234}$ , 7 percent  $U^{238}$ ) normalized per atom of  $U^{235}$  were taken from references 20 and 21. Metal densities were taken from reference 22. A summary of cross sections and densities used in these calculations has been presented in table I.

## Fast Parameters

Mean-square slowing-down length,  $L_f^2$ . - As previously mentioned, mean-square slowing-down lengths were calculated for hydrogenous mixtures by the method of reference 6 in which a formula, equation (108), for  $L_f^2$  is derived taking into account the scattering but not the slowing-down properties of elements other than hydrogen. This introduces small error provided the macroscopic scattering cross section of hydrogen is greater than the macroscopic scattering cross section of the heavy elements in the medium. A limiting form of the rigorous formula, equation (A3) of reference 6, was used for the present calculations since it provides results in good agreement with the more rigorous equation (108) and involves considerably less computational labor.

The values of  $L_f^2$  for water of unit density, by equations (108) and (A3) of reference 6 averaged over the fission spectrum, were calculated as 26.9 and 25.4 square centimeters, respectively. These values compare with the experimentally determined value of  $L_f^2$  for water of 33 square centimeters of reference 23. It is customary in reactor calculations to correct the calculated value of  $L_f^2$  to the experimental value. This multiplicative correction for water from the  $L_f^2$  as calculated by equation (A3) of reference 6 is  $33/25.4 = 1.30$ .

Inasmuch as no experimental data are available for NaOH, the correction factor to the calculated value of  $L_f^2$  for NaOH was determined by ascertaining the mixture of  $H_2O$  and  $Na_2O$  corresponding to NaOH. It was found that a mixture by volume of 40 percent  $H_2O$  of specific gravity 1.00 and 60 percent  $Na_2O$  of specific gravity 2.27 corresponded to NaOH of specific gravity 1.77. Assuming the correction factor to be proportional to the percentage of  $H_2O$  in the mixture, a correction factor of 1.12 was established to apply to all values of  $L_f^2$  as computed from equation (A3) of reference 6. These values of  $L_f^2$  were further corrected to the operating temperature of interest by assuming  $L_f^2$  to be inversely proportional to the square of the density of NaOH.

Macroscopic cross sections. - The remaining fast parameters were calculated from the energy distribution of neutron flux, given by age theory for an infinite medium of the same composition, as the weighting factors on the energy-dependent cross sections (see references 18 and 24). For example, the effective fast macroscopic absorption cross section  $\Sigma_{A,f}$  is given by

$$\Sigma_{A,f} = \frac{\int_{u_{th}}^{\infty} \Sigma'_A(u) \varphi(u) du}{\int_{u_{th}}^{\infty} \varphi'(u) du} \quad (C1)$$

where the flux  $\varphi'(u)$  is obtained as

$$\varphi'(u) = \frac{q(u)}{\xi \Sigma'_T(u)} \quad (C2)$$

and where  $q(u)$  is the age-theory neutron slowing-down density through any energy interval in an infinite medium.

Similarly, the effective fast macroscopic fission cross section  $\Sigma_{F,f}$  and transport mean free path  $\lambda_{TR,f}$  may be evaluated as

$$\Sigma_{F,f} = \frac{\int_0^{u_{th}} \Sigma'_F(u) \varphi'(u) du}{\int_0^{u_{th}} \varphi'(u) du} \quad (C3)$$

$$\lambda_{TR,f} = \frac{\int_0^{u_{th}} \lambda_{TR}'(u) \varphi'(u) du}{\int_0^{u_{th}} \varphi'(u) du} \quad (C4)$$

The fast multiplication constant is therefore given by  $K_f = v \Sigma_{F,f} / \Sigma_{A,f}$ .

The resonance escape probability  $p_{th}$  is the value of  $q$  at thermal energy  $u_{th}$ , inasmuch as a fission spectrum normalized to unity has been employed.

The integrals required are evaluated numerically over the entire fast energy region and in suitably small energy intervals.

#### Thermal Parameters

Macroscopic cross sections. - The thermal parameters of both core and reflector involve macroscopic cross sections which must be suitably averaged over the Maxwellian distribution of neutrons in the thermal region to represent their effective values. For example, in order that the term  $\Sigma_{A,th} \varphi_{th}$  represent the true rate of neutron absorptions occurring per unit volume of reactor,  $\Sigma_{A,th}$  must be some effective

average value if  $\Phi_{th}$  is given as the thermal flux of neutrons corresponding to the most probable speed of the Maxwellian distribution corresponding to energy  $E_{th}$ .

The effective value of  $\Sigma_{A,th}$  averaged over the Maxwellian distribution of neutron flux  $vM(v)$  is given by

$$\Sigma_{A,th} = \frac{\int_0^{\infty} \Sigma'_A vM(v) dv}{\int_0^{\infty} vM(v) dv} \quad (C5)$$

For absorption cross sections which follow the  $1/v$  law, as is usually the case for thermal neutrons, the value of  $\Sigma_{A,th}$  evaluated from equation (C5) turns out to be exactly the local value of  $\Sigma'_A$  corresponding to the average speed of the Maxwellian distribution of neutron density  $M(v)$ . Inasmuch as the average speed is  $\frac{2}{\sqrt{\pi}} = 1.128$  times greater than the most probable speed, the effective value of  $\Sigma_{A,th}$  is 0.886 times the value at the most probable energy to which it is customary to refer measured cross sections. (The pile oscillator values of thermal-absorption cross section used herein have all been referred to the accepted value for gold at the most probable neutron thermal energy).

The same results apply to the macroscopic fission cross section of uranium  $\Sigma_{F,th}$  which very closely follows a  $1/v$  variation for the thermal region.

Similar considerations are made in obtaining an effective value of thermal-transport mean free path  $\lambda_{TR,th}$ . The effective value of  $\lambda_{TR,th}$  is given by

$$\lambda_{TR,th} = \frac{\int_0^{\infty} \lambda'_{TR} vM(v) dv}{\int_0^{\infty} vM(v) dv} \quad (C6)$$

where  $\lambda'_{TR}$  is the local value for neutrons of a particular velocity.

For any particular neutron velocity,  $\Sigma'_{\text{A}}$  and  $\lambda'_{\text{TR}}$  are evaluated as the sum of the products of the reactor atom density of each constituent and the pertinent cross section:

$$\Sigma'_{\text{A}} = N_1 \sigma_{\text{A},1} + N_2 \sigma_{\text{A},2} + \dots + N_n \sigma_{\text{A},n} \quad (\text{C7})$$

$$\frac{1}{\lambda'_{\text{TR}}} = N_1 \sigma_{\text{TR},1} + N_2 \sigma_{\text{TR},2} + \dots + N_n \sigma_{\text{TR},n} \quad (\text{C8})$$

Effect of chemical binding. - The effect of chemical binding of the hydrogen in the molecule for both water and NaOH alters the angular distribution of neutrons scattered by hydrogen. Since this effect occurs almost exclusively in the thermal region and varies rapidly with neutron energy, the average value of the cosine of the scattering angle  $\cos \theta$  as a function of local neutron energy must be known.

In the absence of these specific data, Radkowsky in reference 7 has made use of the "Born approximation" (reference 25) in evaluating an effective value of  $A$ , the atomic mass of the scattering atom, for use in the formula for  $\cos \theta = 2/3A$  applicable for isotropic elastic scattering in the center of mass system. The "Born approximation" indicates the scattering cross section to be proportional to the square of the reduced mass of the neutron and scattering atom. For neutrons of energies well above the region of chemical binding, the hydrogen atom is effectively free and presents a mass of unity and  $\sigma_g$  of 20 barns. Hence, the following proportionality may be formed from which an effective value of  $A$  is determined:

$$\frac{\sigma_{\text{S}'}}{20} = \frac{\left(\frac{A}{A+1}\right)^2}{1/4} \quad (\text{C9})$$

where  $\sigma_{\text{S}'}$  is the local value of hydrogen scattering cross section observed in measurements on water.

By means of equations (C6), (C8), (C9), and the formula  $\cos \theta = 2/3A$ , Radkowsky has checked the experimental values of thermal diffusion length for water for a range of temperature. Effective values of  $\lambda_{\text{TR,th}}$  for the hydroxide reactors herein considered have been numerically evaluated by the same procedure.

The remaining thermal parameters are evaluated as follows:

The thermal multiplication constant  $K_{\text{th}}$  is given by

$$K_{th} = v \frac{\Sigma_{F,th}}{\Sigma_{A,th}}$$

The mean-square thermal diffusion length is given by

$$L^2_{th} = \frac{1}{3} \frac{\lambda_{TR,th}}{\Sigma_{A,th}}$$

APPENDIX D - TEMPERATURE COEFFICIENT OF REACTIVITY AND EXCESS  
URANIUM REQUIREMENTS

The derivation of the first-order perturbation formula presented in appendix I of reference 12 for the two-group two-zone problem has been modified to include the fast fission effect. This modification involves no changes in the derivation procedure of reference 12 and, for this reason, the details of the modified derivation are omitted herein.

The perturbation formula gives the effect of small changes in the nuclear properties of any portion of the reactor volume on the reactivity of the entire reactor. The perturbation formula is herein applied to the problems of determining reactor temperature coefficient of reactivity and excess uranium requirement to overcome burnup and fission-product poisoning.

Perturbation formula. - The two-group neutron diffusion equations for the reactor core are

$$D_f \Delta \Phi_f - (\Sigma_{A,f} + \Sigma_{S,f}) \Phi_f + K_{th} \Sigma_{A,th} \Phi_{th} + K_f \Sigma_{A,f} \Phi_f = 0 \quad (D1)$$

$$D_{th} \Delta \Phi_{th} - \Sigma_{A,th} \Phi_{th} + \Sigma_{S,f} \Phi_f = 0 \quad (D2)$$

where the subscript 0, used to indicate reactor core, has been dropped in this section.

In matrix form, these equations are represented by  $H\Phi = 0$ , where the matrix operator  $H$  is defined as

$$H = \begin{vmatrix} D_{th} \Delta - \Sigma_{A,th} & \Sigma_{S,f} \\ K_{th} \Sigma_{A,th} & D_f \Delta - (\Sigma_{A,f} + \Sigma_{S,f}) + K_f \Sigma_{A,f} \end{vmatrix}$$

and  $\Phi$  is the column matrix

$$\Phi = \begin{vmatrix} \Phi_{th} \\ \Phi_f \end{vmatrix}$$

The operator  $H$  defined herein includes the fast fission term  $K_f \Sigma_{A,f}$  which was taken as zero in reference 12.

The adjoint matrix  $H^*$ , obtained by reflection of all elements of  $H$  about its principal diagonal, is given by

$$H^* = \begin{vmatrix} D_{th}\Delta - \Sigma_{A,th} & K_{th} \Sigma_{A,th} \\ \Sigma_{S,f} & D_f\Delta - (\Sigma_{A,f} + \Sigma_{S,f}) + K_f \Sigma_{A,f} \end{vmatrix}$$

The adjoint matrix equation defining the adjoint functions is then  $H^* \Psi^+ = 0$  and the adjoint equations are given by

$$D_f \Delta \Psi_f^+ - (\Sigma_{A,f} + \Sigma_{S,f}) \Psi_f^+ + K_f \Sigma_{A,f} \Psi_f^+ + \Sigma_{S,f} \Psi_{th}^+ = 0 \quad (D3)$$

$$D_{th} \Delta \Psi_{th}^+ - \Sigma_{A,th} \Psi_{th}^+ + K_{th} \Sigma_{A,th} \Psi_f^+ = 0 \quad (D4)$$

The addition of the term  $K_f \Sigma_{A,f}$  in the second-row second-column element of the operator matrices  $H$  and  $H^*$  introduces no change in the detailed derivation of the perturbation formula given in appendix I of reference 12. Hence, only the final formulas are presented herein.

The perturbation formula, written in terms of the neutron fluxes  $\Psi_{th}$  and  $\Psi_f$  and their adjoint functions  $\Psi_{th}^+$  and  $\Psi_f^+$ , is:

$$P = \frac{\int_{\substack{\text{reactor} \\ \text{volume}}} (\Psi_{th}^+ \Psi_f^+) \begin{vmatrix} \delta_a & \delta_b \\ \delta_c & \delta_d \end{vmatrix} \begin{vmatrix} \Psi_{th} \\ \Psi_f \end{vmatrix} d\tau}{\int_{\text{core}} (K_{th} \Sigma_{A,th} \Psi_{th} \Psi_f^+ + K_f \Sigma_{A,f} \Psi_f \Psi_f^+) d\tau} \quad (D5)$$

where

$$\delta_a = \delta \left[ D_{th}\Delta - \Sigma_{A,th} \right]$$

$$\delta_b = \delta \left[ \Sigma_{S,f} \right]$$

$$\delta_c = \delta \left[ K_{th} \Sigma_{A,th} \right]$$

$$\delta_d = \delta \left[ D_f\Delta - (\Sigma_{A,f} + \Sigma_{S,f}) + K_f \Sigma_{A,f} \right]$$

If the indicated matrix operations are performed and  $P$  expressed in terms of the various contributions to the reactivity due to the individual changes in the pertinent nuclear constants, the following results are obtained:

$$P = P(D_{th}) + P(D_f) + P(\Sigma_{A,F}) + P(\Sigma_{S,f}) + P(\Sigma_{A,th}) + P(v\Sigma_{F,f}) + P(v\Sigma_{F,th}) \quad (D6)$$

where

$$P(D_{th}) = \frac{- \int_{vol} \nabla \varphi_{th}^+ \cdot \nabla \varphi_{th} \delta(D_{th}) d\tau}{Y} \quad (D7)$$

$$P(D_f) = \frac{- \int_{vol} \nabla \varphi_f^+ \cdot \nabla \varphi_f \delta(D_f) d\tau}{Y} \quad (D8)$$

$$P(\Sigma_{A,f}) = \frac{- \int_{vol} \varphi_f^+ \varphi_f \delta(\Sigma_{A,f}) d\tau}{Y} \quad (D9)$$

$$P(\Sigma_{S,f}) = \frac{- \int_{vol} (\varphi_{th}^+ \varphi_f - \varphi_f^+ \varphi_f) \delta(\Sigma_{S,f}) d\tau}{Y} \quad (D10)$$

$$P(\Sigma_{A,th}) = \frac{- \int_{vol} \varphi_{th}^+ \varphi_{th} \delta(\Sigma_{A,th}) d\tau}{Y} \quad (D11)$$

$$P(v\Sigma_{F,th}) = \frac{- \int_{vol} \varphi_f^+ \varphi_{th} \delta(v\Sigma_{F,th}) d\tau}{Y} \quad (D12)$$

$$P(v\Sigma_{F,f}) = \frac{- \int_{vol} \varphi_f^+ \varphi_f \delta(v\Sigma_{F,f}) d\tau}{Y} \quad (D13)$$

$$Y = \int_{\text{core}} (v \Sigma_{F,\text{th}} \varphi_{\text{th}} \varphi_f^+ + v \Sigma_{F,f} \varphi_f \varphi_f^+) d\tau$$

Adjoint equations. - For use in the perturbation formula, the adjoint functions  $\varphi_f^+$  and  $\varphi_{\text{th}}^+$  must be known as a function of position (radius  $r$ , in this case).

2525

Equations (3) and (4) are the core adjoint equations.

$$D_{f,0} \Delta \varphi_{f,0}^+ - (\Sigma_{A,f,0} + \Sigma_{S,f,0}) \varphi_{f,0}^+ + K_f \Sigma_{A,f,0} \varphi_{f,0}^+ + \Sigma_{S,f,0} \varphi_{\text{th},0}^+ = 0 \quad (D3)$$

$$D_{\text{th},0} \Delta \varphi_{\text{th},0}^+ - \Sigma_{A,\text{th},0} \varphi_{\text{th},0}^+ + K_{\text{th}} \Sigma_{A,\text{th},0} \varphi_{f,0}^+ = 0 \quad (D4)$$

The reflector adjoint equations, obtained in the same manner as for the core, are

$$D_{f,1} \Delta \varphi_{f,1}^+ - (\Sigma_{A,f,1} + \Sigma_{S,f,1}) \varphi_{f,1}^+ + \Sigma_{S,f,1} \varphi_{\text{th},1}^+ = 0 \quad (D14)$$

$$D_{\text{th},1} \Delta \varphi_{\text{th},1}^+ - \Sigma_{A,\text{th},1} \varphi_{\text{th},1}^+ = 0 \quad (D15)$$

In the derivation of the perturbation formula, the same boundary conditions are applied to the adjoint functions as are applied to the fluxes, namely:

$$\left. \begin{array}{l} \varphi_{f,0}^+ = \varphi_{f,1}^+ \\ \varphi_{\text{th},0}^+ = \varphi_{\text{th},1}^+ \\ D_{f,0} \nabla \varphi_{f,0}^+ = D_{f,1} \nabla \varphi_{f,1}^+ \\ D_{\text{th},0} \nabla \varphi_{\text{th},0}^+ = D_{\text{th},1} \nabla \varphi_{\text{th},1}^+ \end{array} \right\} \text{at core-reflector interface}$$

$$\varphi_{f,1}^+ = \varphi_{\text{th},1}^+ = 0 \quad \text{at reflector outer surface}$$

$$\left[ \varphi_f^+ \right]_{\text{all } r}, \left[ \varphi_{\text{th}}^+ \right]_{\text{all } r} < \infty$$

The solution of the adjoint equations subject to the foregoing boundary conditions is identical, in procedure, to the solution of the neutron flux equations subject to the same boundary conditions.

Temperature coefficient of reactivity. - The procedure used for determining the differential changes in the pertinent nuclear parameters with temperature, required for use in the perturbation formula, is presented herein.

For the fast parameters, two principal effects of change in temperature are accounted for:

Effect A - accounts for change in neutron energy range constituting the fast group.

Effect B - accounts for change in density and hence in density of nuclei of NaOH in reactor core only inasmuch as uranium and structural material remain fixed in the reactor.

The relations for the fast parameters are

$$\frac{d\Sigma_{A,f}}{dT} = \frac{d\Sigma_{A,f}}{du_{\text{th}}} \frac{du_{\text{th}}}{dT} \quad (\text{D16})$$

$$\frac{d\Sigma_{F,f}}{dT} = \frac{d\Sigma_{F,f}}{du_{\text{th}}} \frac{du_{\text{th}}}{dT} \quad (\text{D17})$$

$$\frac{d\lambda_{\text{TR},f}}{dT} = \frac{d\lambda_{\text{TR},f}}{du_{\text{th}}} \frac{du_{\text{th}}}{dT} - \lambda_{\text{TR},f} \frac{d\rho_m}{\rho_m dT} \quad (\text{D18})$$

$$\frac{d\Sigma_{S,f}}{dT} = \Sigma_{S,f} \frac{d\rho_m}{\rho_m dT} \quad (\text{D19})$$

In relations (D16) to (D18), the respective values of  $d/du_{\text{th}}$  are obtained from equations (C1), (C3), and (C4); the subscript  $m$  refers to the moderator.

Effect B is neglected in equations (D16) and (D17) because the fast absorption by NaOH is small. Effect A is negligible in comparison to effect B in the neutron slowing-down process and hence is neglected

in equation (D19). Effect B is included in equations (D18) and (D19) in a manner implying that the diffusion and slowing-down processes are due primarily to the NaOH.

For the thermal parameters, two principal effects of change in temperature are accounted for:

Effect B - same as for fast parameters.

2525

Effect C - accounts for change in microscopic cross sections with change in thermal temperature.

For all nuclei within the reactor excepting  $Xe^{135}$ , the microscopic absorption cross section  $\sigma_A$  is assumed to follow the  $1/v$  law in the vicinity of thermal energy. Hence, for these nuclei  $\sigma_A$  is inversely proportional to  $\sqrt{T}$  so that

$$\frac{d\sigma_{A,th}}{\sigma_{A,th}} = - \frac{dT}{2T}$$

For  $Xe^{135}$ , a quantity  $\alpha^{Xe}$  which is a function of temperature is defined as

$$\alpha^{Xe} = \frac{d\sigma_A^{Xe}}{dT}$$

The relations for the thermal parameters are

$$\frac{d\lambda_{TR,th}}{dT} = -\lambda_{TR,th,m} \frac{d\rho_m}{\rho_m dT} - \lambda_{TR,th} \frac{d\sigma_{TR,th}}{\sigma_{TR,th} dT} \quad (D20)$$

$$\frac{d\Sigma_{A,th}}{dT} = \Sigma_{A,th,m} \frac{d\rho_m}{\rho_m dT} + \Sigma_{A,th} \left( \frac{1}{2T} \right) + N^{Xe} \alpha^{Xe} \quad (D21)$$

$$\frac{d(K_{th} \Sigma_{A,th})}{dT} = K_{th} \Sigma_{A,th} \left( -\frac{1}{2T} \right) \quad (D22)$$

The foregoing changes in nuclear parameters are assumed to be homogeneously distributed over the entire reactor core. No changes in the reflector parameters are taken as contributing to change in reactivity.

Estimate of excess uranium requirements. - Use of the perturbation formula to calculate the additional uranium required to counteract the effects of fission-product poisoning and uranium burnup is described herein. The principal poisons are  $Xe^{135}$  and  $Sm^{149}$ ; a host of other fission-fragment poisons appear and are accounted for by the assumption that for every uranium atom fissioned the equivalent of a single poison atom appears with a microscopic absorption cross section  $\sigma_{A,th}^P$  equal to 100 barns.

The excess uranium requirement is given by the relation stating that the reactivity decrease due to accumulation of fission-product poison and due to fuel burnup must equal the reactivity increase brought about by addition of extra fuel.

2525

The assumptions used in the calculation of these reactivity changes are as follows:

- (1) Introduction of the fission poisons affects only  $\Sigma_{A,th}$ .
- (2) Only the uranium thermal absorption and production parameters are affected by subtraction or introduction of uranium into the reactor core. This assumption implies that the reactor is principally thermal.
- (3) The fission poisons and added uranium are assumed to be distributed uniformly over the volume of the reactor core.

Let:

$\delta N^U$  number of uranium atoms per cubic centimeter of reactor core burned up during the required reactor operation.

$N^U$  uranium concentration required for the hot unpoisoned reactor (Investment corresponding to this concentration is given by the criticality calculations.)

$\beta$  fractional increase in uranium concentration, over that calculated for the hot unpoisoned reactor, to counteract reactivity effects associated with fission product poisoning and fuel burnup.

The weighting factors in the expression for the change in reactivity  $P$ , are evaluated as follows:

- (a) To calculate the reactivity decrease due to poison,  $P(\Sigma_{A,th})$  (equation (D11)) is evaluated by taking

$$\delta(\Sigma_{A,th}) = N^{Xe} \sigma_{A,th}^{Xe} + N^{Sm} \sigma_{A,th}^{Sm} + (\delta N^U) \sigma_{A,th}^P$$

(b) To calculate the reactivity decrease due to fuel burnup,  $P(\Sigma_{A,th})$  (equation (D11)) is evaluated by taking

$$\delta(\Sigma_{A,th}) = -(\delta N^U) \sigma_{A,th}^U$$

and  $Pv\Sigma_{F,th}$  (equation (D12)) is evaluated by taking

$$\delta(v\Sigma_{F,th}) = -v(\delta N^U) \sigma_{F,th}^U$$

(c) To calculate the reactivity increase due to the addition of uranium in excess of that required for criticality of the hot unpoisoned reactor,  $P(\Sigma_{A,th})$  (equation (D11)) is evaluated by taking

$$\delta(\Sigma_{A,th}) = \beta N^U \sigma_{A,th}^U$$

and  $P(v\Sigma_{F,th})$  (equation (D12)) is evaluated by taking

$$\delta(v\Sigma_{F,th}) = v\beta N^U \sigma_{F,th}^U$$

#### REFERENCES

1. Anon.: A Circulating Fuel Prototype for the Aircraft Reactor Experiment. H. K. Ferguson Co., HKF-106, June 19, 1950.
2. Anon.: Homogeneous Reactor for Subsonic Aircraft. H. K. Ferguson Co., HKF-109, Dec. 15, 1950.
3. Anon.: Circulating Moderator-Coolant Reactor for Subsonic Aircraft. H. K. Ferguson Co., HKF-112, Aug. 29, 1951.
4. Greuling, E., Spinrad, B., and Masket, A. V.: Critical Mass and Neutron Distribution Calculations for the  $H_2O$  Moderated Reactor with  $D_2O$ ,  $H_2O$ , and Be Reflectors. MonP-402, Oct. 29, 1947.
5. Watt, B. E.: Energy Spectrum of Neutrons from Fissions Induced by Thermal Neutrons. LA-718, Dec. 17, 1948.
6. Marshak, Robert E.: Theory of the Slowing Down of Neutrons by Elastic Collision with Atomic Nuclei. Rev. Mod. Phys. vol. 19, no. 3, July, 1947, pp. 185-238.

7. Radkowsky, A.: Temperature Dependence of Thermal Transport Mean Free Path. Quarterly Report, April, May, and June 1950. Physics Division ANL-4476, July 5, 1950, pp. 89-100.

8. Adair, R. K.: Neutron Cross Sections of the Elements. Rev. Modern Phys., vol. 22, no. 3, July 1950, pp. 249-289.

9. Webster, J. W.: Xe Effect in an Epi-Thermal Reactor. Y-F10-17- Oct. 10, 1950.

10. Glasstone, Samuel, and Edlund, Milton C.: The Elements of Nuclear Reactor Theory. Part III - Tech. Information Div., Oak Ridge. TID-386, Nov. 1950.

11. Arndt, Kurt and Ploetz, George.: Conductivity and Viscosity of Molten NaOH and KOH. Y-F35-5 (Translation for Z. fur Physikalische Chemie 121, 439-455, March 21, 1952).

12. Garabedian, H. L.: Theory of Homogeneous Control of a Cylindrical Reactor. Westinghouse Electric Corp. WAPD-19, Sept. 20, 1950.

13. Bogart, Donald: Estimation of Neutron Energy for First Resonance from Absorption Cross Section for Thermal Neutrons. NACA RM E51G03, 1951.

14. Wachtel, William W., and Rom, Frank E.: Analysis of the Liquid-Metal Turbojet Cycle for Propulsion of Nuclear Powered Aircraft. NACA RM E51D30, 1951.

15. Anon.: Metals Handbook, 1948 Edition. Am. Soc. Metals, (Cleveland) 1948, p. 314.

16. McCready, Robert R., Spooner, Robert B., and Valerino, Michael F.: Distribution of Fissionable Material in Thermal Reactors of Spherical Geometry for Uniform Power Generation. NACA RM E52C11, 1952.

17. Weinberg, Alvin M., and Noderer, L. C.: Theory of Neutron Chain Reactions. vol. II, Part I, CF-51-5-98, Aug. 10, 1951.

18. Anon.: Criticality and Control - NEPA Technical Report No. 6. Fairchild Engine and Airplane Corp., Oct. 1, 1948.

19. Pomerance, H.: Thermal Neutron Capture Cross Sections. Phys. Rev., vol. 83, no. 3, Aug. 1, 1951.

20. Ehrlich, R.: Multi-group and Adjoint Calculations for SAPL-5. KAPL-346, May 10, 1950.

2525

2525

21. Smith, Nicholas, M., Jr.: KAPL Cross Section Curves for Xe-135, U-235, and U-238. Y-F10-51, April 17, 1951.
22. Anon.: Handbook of Chemistry and Physics. C. D. Hodgman, Ed. Chem. Rubber Pub. Co. (Cleveland), 32d, ed., 1949.
23. Hill, J. E., Roberts, L. D., and Fitch, T. E.: The Slowing Down Distribution from a Point Source of Fission Neutrons in Light Water. ORNL-181, Dec. 10, 1948.
24. Spooner, Robert B.: Comparison of Two-Group and Multigroup Reactor Solutions for Some Reflected Intermediate Assemblies. NACA RM E52D04, 1952.
25. Bethe, H. A.: Nuclear Physics. B. Nuclear Dynamics, Theoretical. Rev. Modern Phys., vol. 9, no. 2, April, 1937, pp 69-244.

TABLE I - NUCLEAR PROPERTIES OF REACTOR MATERIALS



Material	Core		Reflector	
	Density (gm/cc)	Nuclei per cc	Density (gm/cc)	Nuclei per cc
NaOH	1.57	$0.0236 \times 10^{24}$	1.58	$0.0238 \times 10^{24}$
Na	.74	.0194	----	----
Ni	8.90	.0913	----	----
Fe	7.85	.0847	----	----
U	18.7	.0473	----	----

Atom	Thermal neutron cross sections <sup>a</sup> (barns)		
	Absorption $\sigma_A$	Scattering $\sigma_S$	Fission $\sigma_F$
Na	0.24	3.0	---
O	.0005	3.9	---
H	.17	reference 7	---
Ni	2.34	17.3	---
Fe	1.24	10.9	---
U	299	12.0	250

<sup>a</sup>Thermal energy  $E_{th} = 0.092$  ev corresponding to an average temperature of  $1450^{\circ}$  F.

TABLE II - TWO-GROUP THEORY REACTOR CONSTANTS

## (a) Core.

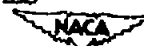


Reactor	$R = \frac{N_U}{N}$	$\lambda_{TR,f,0}$ (cm)	$\lambda_{TR,th,0}$ (cm)	$L^2_{f,0}$ (cm <sup>2</sup> )	$L^2_{th,0}$ (cm <sup>2</sup> )	$K_f$	$K_{th}$	$P_{th,0}$
I	50	3.580	1.624	102.0	4.528	1.581	1.717	0.516
	100	3.589	1.630	102.0	7.365	1.385	1.456	.685
	200	3.594	1.634	102.0	11.312	1.076	1.115	.788
II	50	3.858	1.784	105.6	5.066	1.658	1.830	0.533
	150	3.884	1.795	105.6	12.204	1.334	1.461	.776
	300	3.895	1.798	105.6	18.769	1.104	1.121	.854
III	100	4.087	1.902	104.9	9.854	1.665	1.832	0.729
	400	4.123	1.910	104.9	28.765	1.283	1.532	.902
IV	50	3.766	1.723	89.2	4.299	1.750	1.961	0.549
	500	3.839	1.740	89.2	27.611	1.213	1.247	.917

## (b) Reflector.

$\lambda_{TR,f,1}$ (cm)	$\lambda_{TR,th,1}$ (cm)	$L^2_{f,1}$ (cm <sup>2</sup> )	$L^2_{th,1}$ (cm <sup>2</sup> )	$P_{th,1}$
3.820	1.727	86.4	67.2	0.970

TABLE III - NUCLEAR PROPERTIES OF FUEL-ELEMENT ALLOYING MATERIALS



Element	Density (gm/cc) (68° F)	Nuclei per cc N	Thermal neutron cross sections (0.025 ev) (barns)		Thermal macroscopic cross sections $\Sigma = N\sigma$ (0.025 ev) (cm <sup>-1</sup> )		Effective <sup>a</sup> thermal macroscopic cross sections (0.092 ev) (cm <sup>-1</sup> )	
			$\sigma_A$	$\sigma_S$	$\Sigma_A$	$\Sigma_S$	$\Sigma_{A_{th}}$	$\Sigma_{S_{th}}$
Ni	8.9	$0.0913 \times 10^{24}$	4.5	17	0.41	1.6	0.189	1.6
Fe	7.85	.0847	2.4	11	.20	.93	.093	.93
Ti	4.5	.0566	5.8	6	.33	.34	.152	.34
V	5.96	.0705	4.7	7	.33	.49	.153	.49
Cr	6.92	.0801	2.8	4	.22	.32	.103	.32
Cb	8.4	.0545	1.1	7	.06	.38	.028	.38
Mo	10.2	.0640	2.4	7	.15	.45	.071	.45
Co	8.7	.0890	36	5	3.20	.44	1.48	.44
W	19.3	.0632	18	5	1.14	.32	.526	.32

<sup>a</sup>Averaged over Maxwellian distribution of neutron flux.

TABLE IV - EXCESS URANIUM REQUIREMENTS AND TEMPERATURE COEFFICIENT OF REACTIVITY FOR NaOH-COOLED AND MODERATED REACTORS. OPERATING POWER, 500,000 KILOWATTS; OPERATING TIME 24 HOURS



NACA RM E52119

Reactor I. Core composition: NaOH, 0.82; Ni, 0.08; Na, 0.10.				Reactor III. Core composition: NaOH, 0.90; Na, 0.10.				
Parameter	$\frac{d(\text{Param})}{dT}$	$\frac{dp}{dT}$	$\frac{d(\text{Param})}{dT}$	$\frac{dp}{dT}$	$\frac{d(\text{Param})}{dT}$	$\frac{dp}{dT}$	$\frac{d(\text{Param})}{dT}$	$\frac{dp}{dT}$
$\frac{1}{5} \lambda_{MR,th}$	+0.03142	-0.06620	+0.03147	-0.05115	+0.03239	+0.05167	+0.03239	-0.04107
$\Sigma_{A,th}$	-0.4244	+0.31848	-0.4141	+0.31988	-0.4213	+0.31474	-0.5769	+0.32737
$K_{th} \Sigma_{A,th}$	-0.4304	-0.31638	-0.4152	-0.31957	-0.4323	-0.31540	-0.5850	-0.32461
$\frac{1}{3} \lambda_{MR,f}$	+0.3208	-0.4228	+0.3209	-0.4105	+0.3214	-0.4176	+0.3241	-0.4207
$\Sigma_{A,f}$	-0.6790	+0.4380	-0.6503	+0.4337	-0.5101	+0.4263	-0.6257	+0.4144
$\Sigma_{S,f}$	-0.5190	-0.4372	-0.5191	-0.4126	-0.5191	-0.4340	-0.5211	-0.4273
$K_f \Sigma_{A,f}$	-0.5116	-0.4558	-0.5549	-0.4368	-0.5203	-0.4526	-0.6340	-0.4191
Net $\frac{dp}{dT}$		-0.4575		-0.4242		-0.4629		-0.4348
$\Sigma_{A,th}$ without poison	-0.4223	+0.31691	-0.4134	+0.31890	-0.4194	+0.31344	-0.5728	+0.32591
Net $\frac{dp}{dT}$		-0.4731		-0.4340		-0.4758		-0.4504



TABLE V - SUMMARY OF REPRESENTATIVE NUCLEAR-POWERED-AIRPLANE DATA FOR VARIOUS FLIGHT CONDITIONS

Flight conditions	50,000		30,000		50,000		30,000	
Altitude, ft	0.9		0.9		1.5		1.5	
Mach number	18.0		18.0		6.5		6.5	
Lift-drag ratio								
Turbojet operating conditions								
Air heat-exchanger wall temperature, °F	1000		1000		1000		1000	
Optimum turbine-inlet temperature, °F	820		860		900		880	
Optimum compressor pressure ratio	5.2		4.4		2.4		2.2	
Component weights								
Reactor, shield, payload, auxiliaries, lb	100,000	150,000	100,000	150,000	100,000	150,000	100,000	150,000
Engines and air heat exchangers, lb	40,000	60,000	12,000	18,000	110,000	165,000	28,000	42,000
Airplane structure, lb	80,000	90,000	48,000	72,000	90,000	135,000	55,000	85,000
Airplane gross weight, lb	200,000	300,000	160,000	240,000	300,000	450,000	183,000	275,000
Total engine air flow, lb/sec	480	735	400	600	2500	3450	1720	2580
Total engine air flow corrected to static sea-level conditions, lb/sec	2570	3560	785	1150	5370	8600	1700	2250
Number engines of 300 lb/sec corrected air flow	8	12	3	4	20	30	6	9
Reactor conditions <sup>a</sup>								
Heat release, kw	70,000	105,000	60,000	90,000	340,000	510,000	270,000	405,000
Fuel element sandwich thickness, in.	0.012	0.012	0.012	0.012	0.012	0.012	0.012	0.012
NaOH coolant velocity, ft/sec	15	15	15	15	15	15	15	15
Reactor length and diameter, ft	2.0	2.5	2.0	2.5	2.0	2.5	2.0	2.5
Fuel-element volume fraction	0.12	0.08	0.12	0.06	0.12	0.06	0.12	0.06
Equivalent diameter of flow passage, in.	0.18	0.38	0.18	0.38	0.18	0.38	0.18	0.38
Fuel-element maximum temperature, °F	1135	1140	1155	1160	1150	1135	1145	1150
NaOH temperature into reactor, °F	1086	1090	1075	1065	1085	1090	1080	1085
NaOH temperature out of reactor, °F	1115	1110	1125	1115	1115	1110	1120	1115
Uranium investment (Inconel fuel elements), lb	44	38	44	38	44	59	44	39
Uranium investment (stainless steel elements), lb	35	33	35	33	35	35	35	33

<sup>a</sup>Reactors are reflected by 6 inches of NaOH and operate at uniform wall temperature. Difference between average NaOH temperature and air heat-exchanger effective wall temperature taken as 100° F.

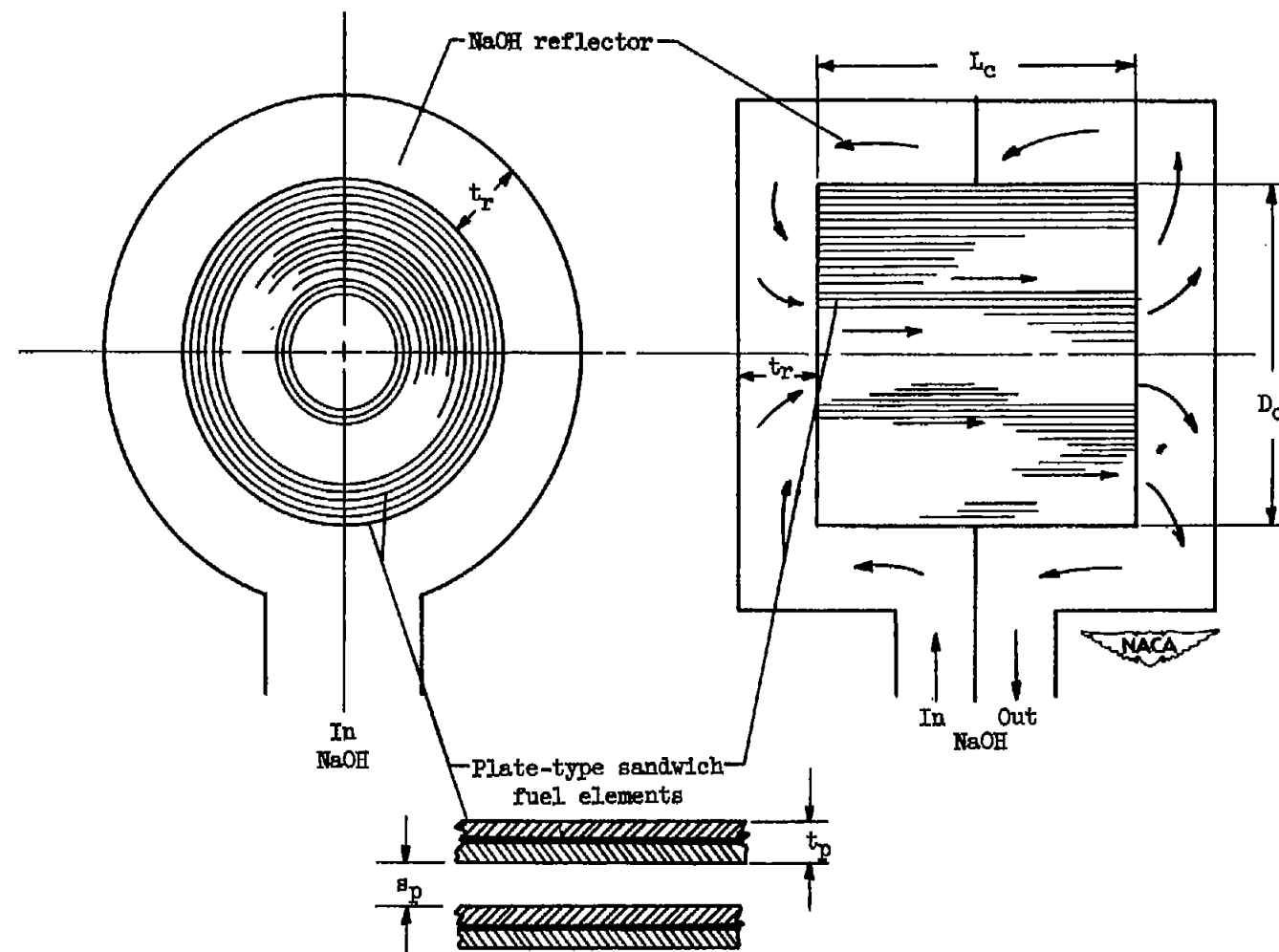


Figure 1. - Schematic diagram of NaOH-cooled, moderated, and reflected reactor and typical heat-transfer configuration.

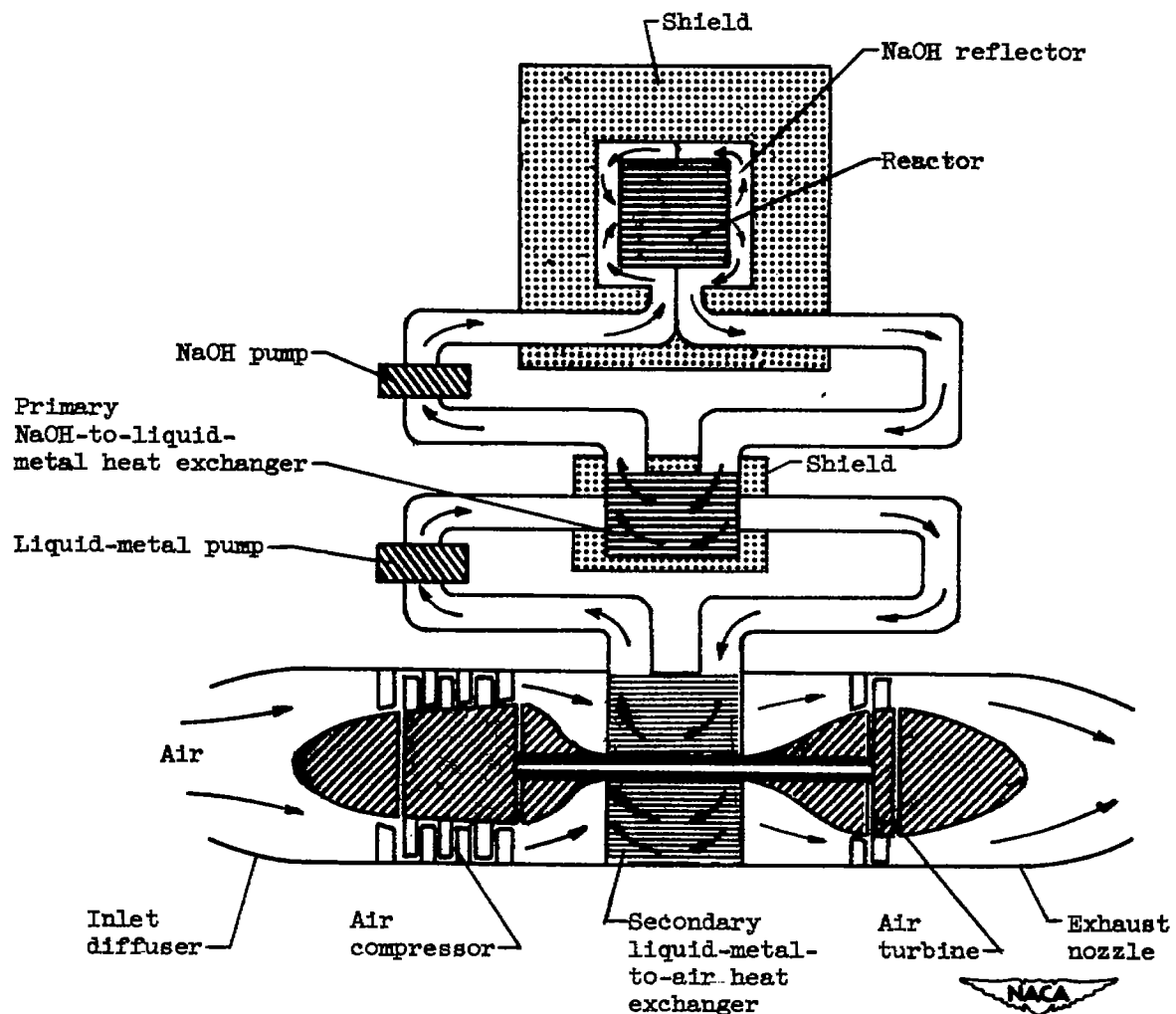


Figure 2. - Schematic diagram of nuclear-powered turbojet engine. Primary coolant, NaOH; secondary coolant, liquid metal.

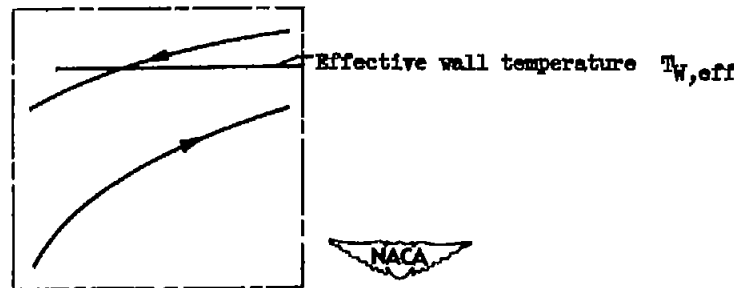
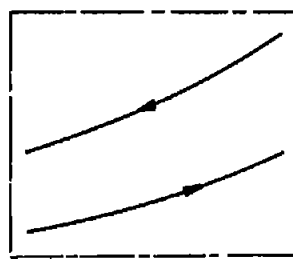
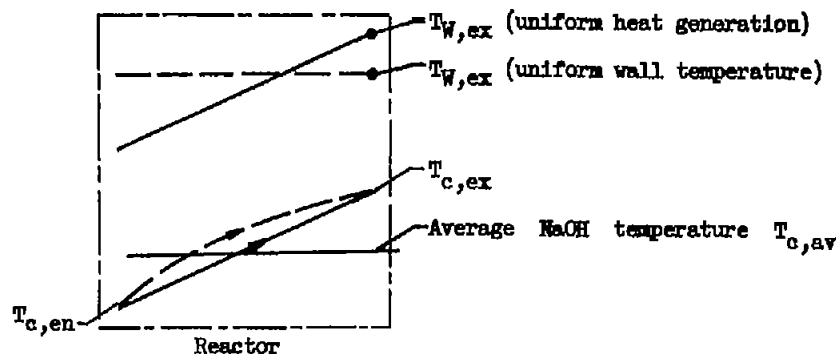
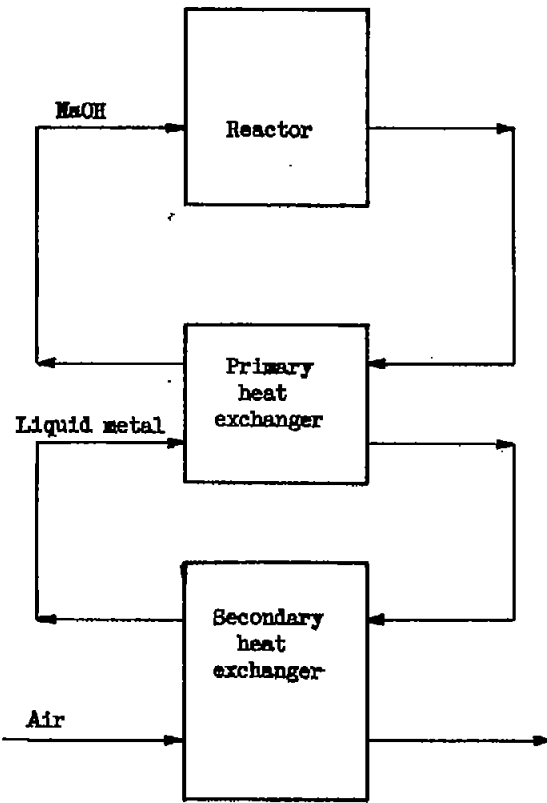
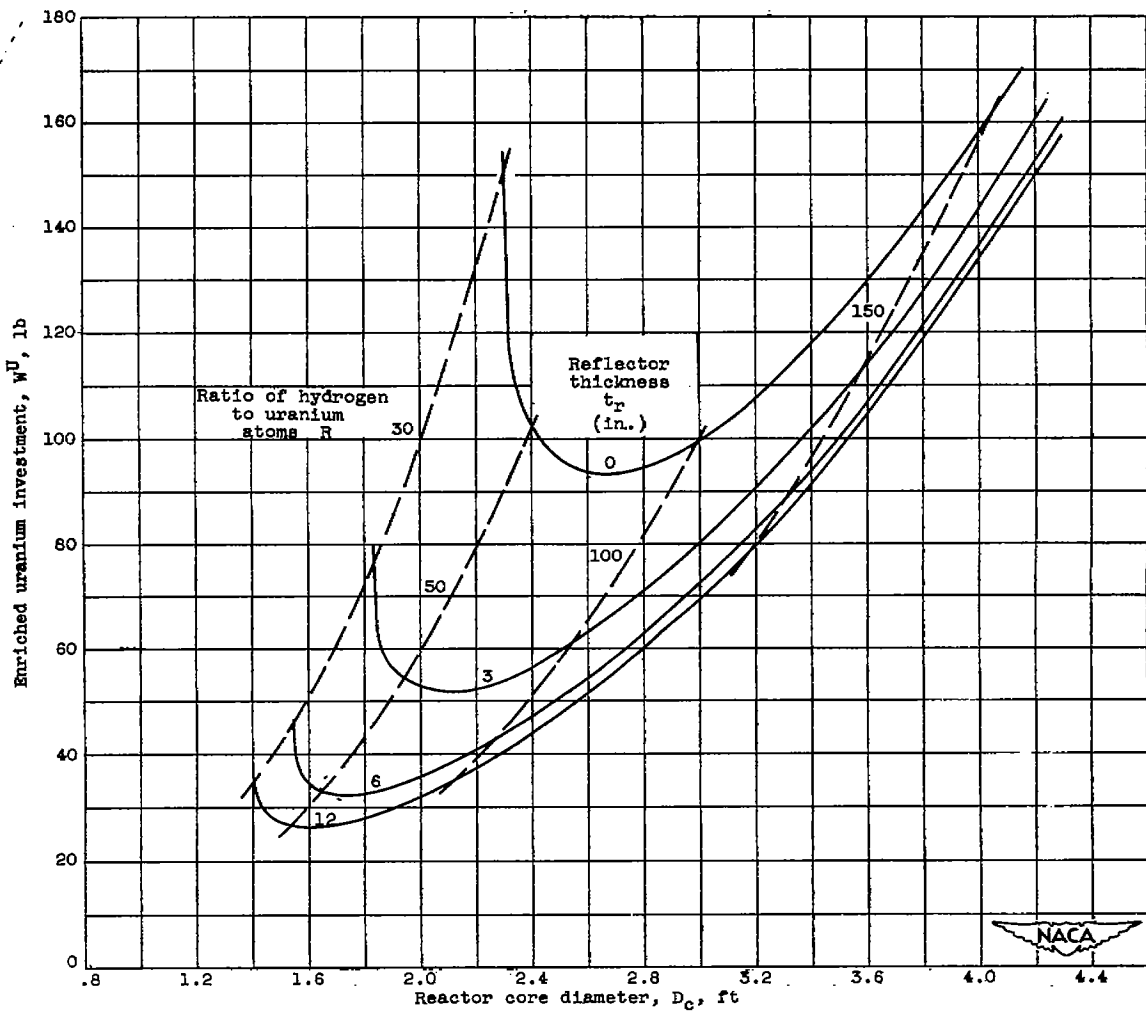


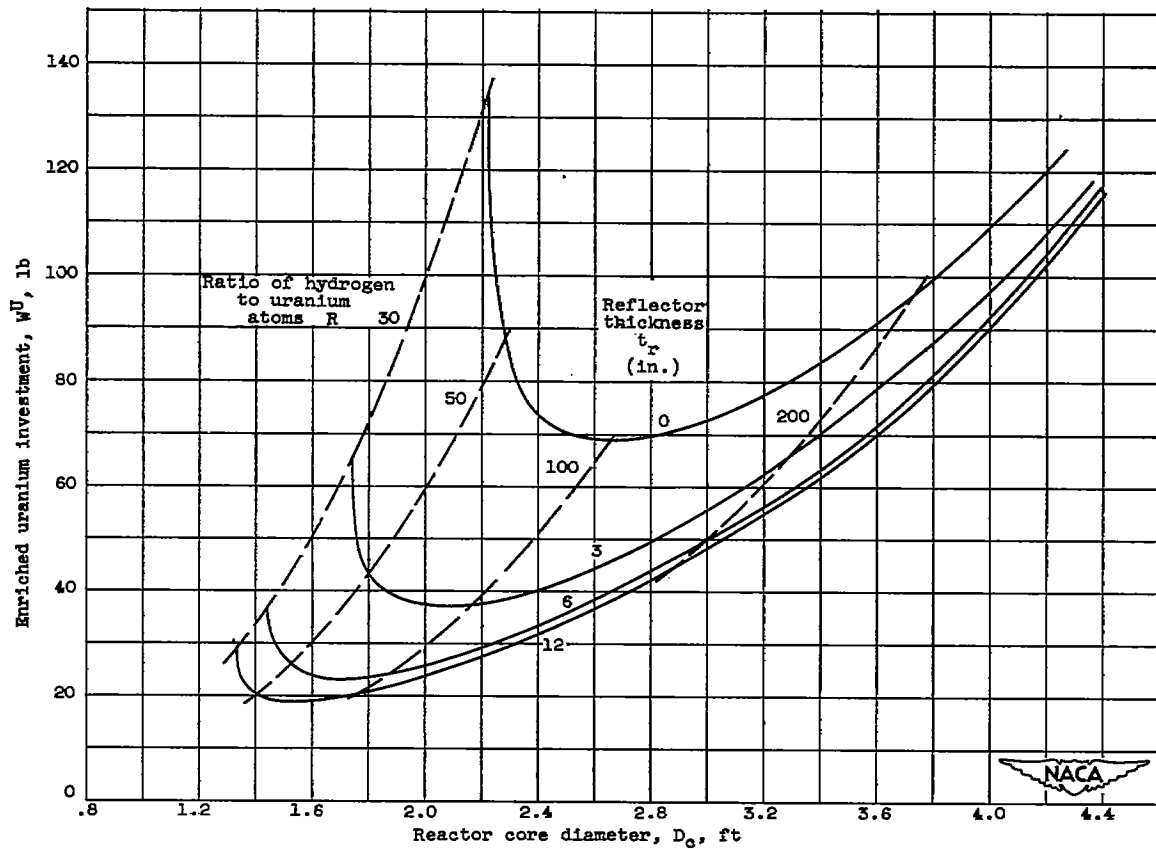
Figure 3. - Schematic diagram of heat-exchanger system and relative temperature distributions.



(a) Reactor I. Core composition: NaOH, 0.82; Ni, 0.08; Na, 0.10.

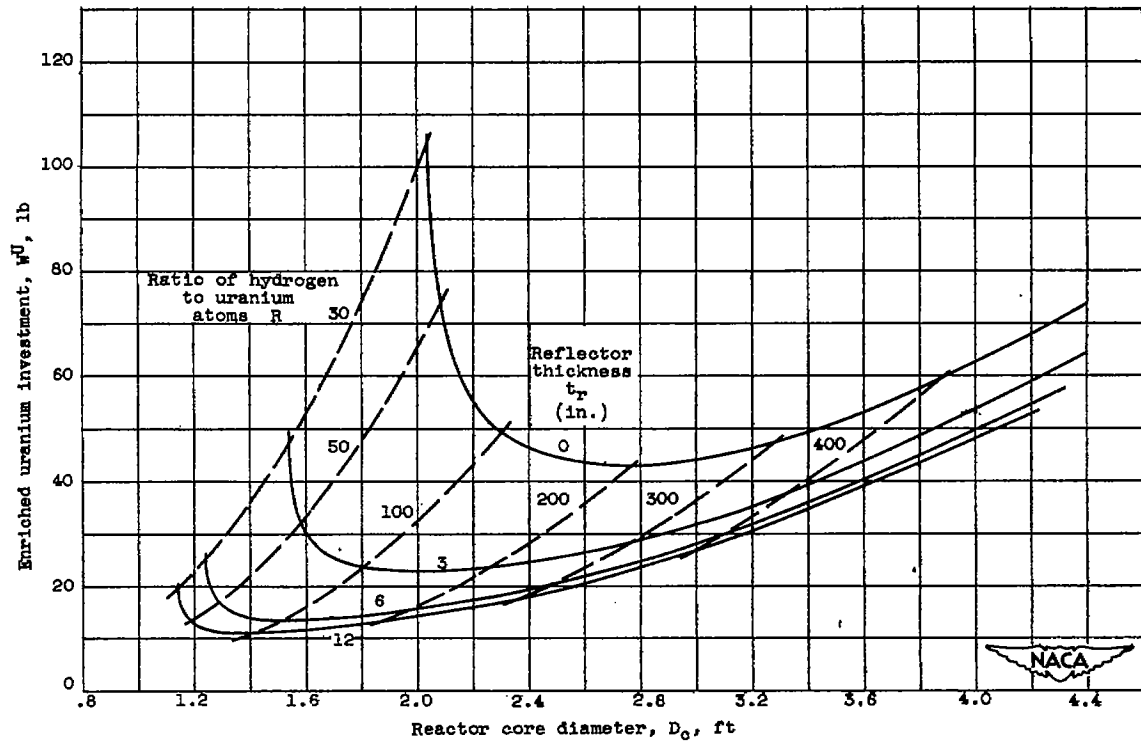
Figure 4. - Enriched uranium investment for NaOH-cooled, moderated, and reflected reactors. Length-diameter ratio of cylindrical core, 1.0; average Moderator temperature, 1450° F.

2525



(b) Reactor II. Core composition: NaOH, 0.82; Fe, 0.08; Na, 0.10.

Figure 4. - Continued. Enriched uranium investment for NaOH-cooled, moderated, and reflected reactors. Length-diameter ratio of cylindrical core, 1.0; average moderator temperature, 1450° F.



(c) Reactor III. Core composition: NaOH, 0.90; Na, 0.10.

Figure 4. - Continued. Enriched uranium investment for NaOH-cooled, moderated, and reflected reactors. Length-diameter ratio of cylindrical core, 1.0; average moderator temperature,  $1450^\circ$  F.

2525

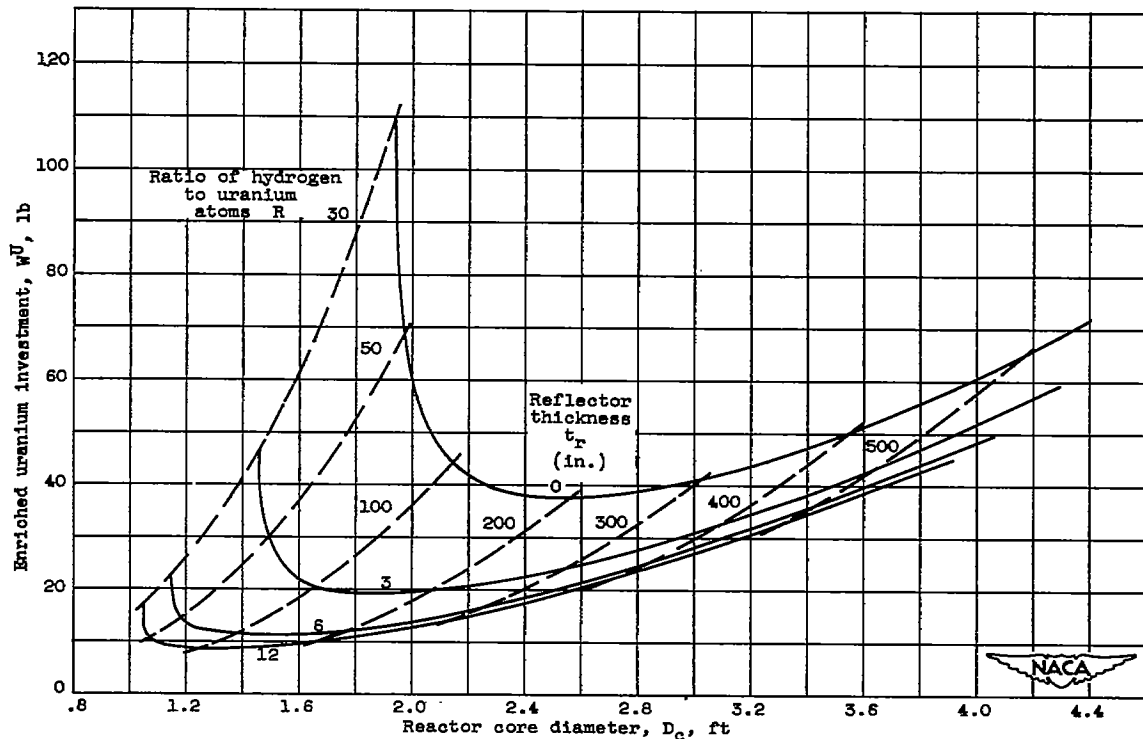


Figure 4. - Concluded. Enriched uranium investment for NaOH-cooled, moderated, and reflected reactors. Length-diameter ratio of cylindrical core, 1.0; average moderator temperature, 1450° F.

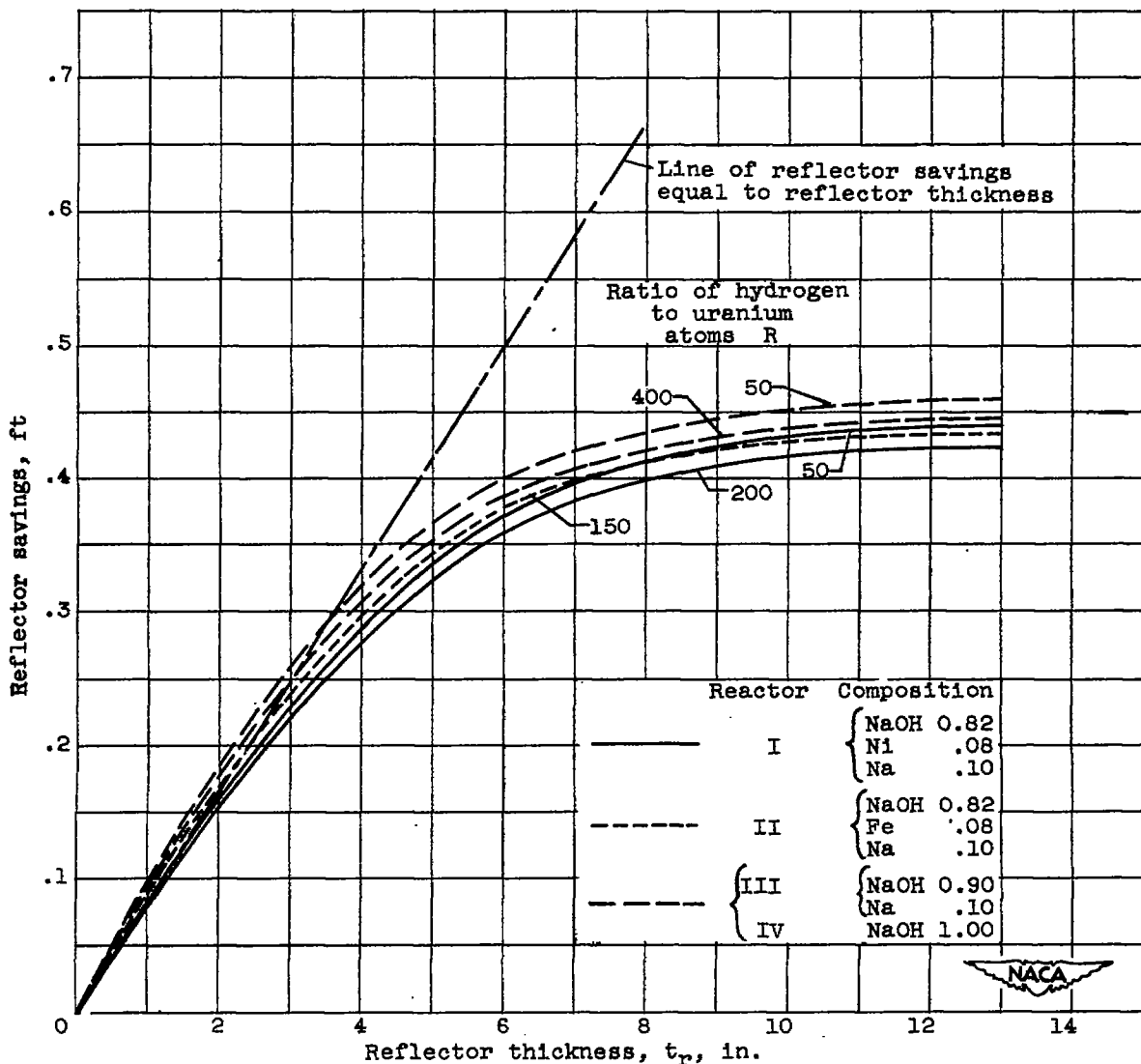


Figure 5. - Representative reflector savings for NaOH-cooled, moderated, and reflected reactors. Average reflector temperature,  $1400^{\circ}$  F.

2525

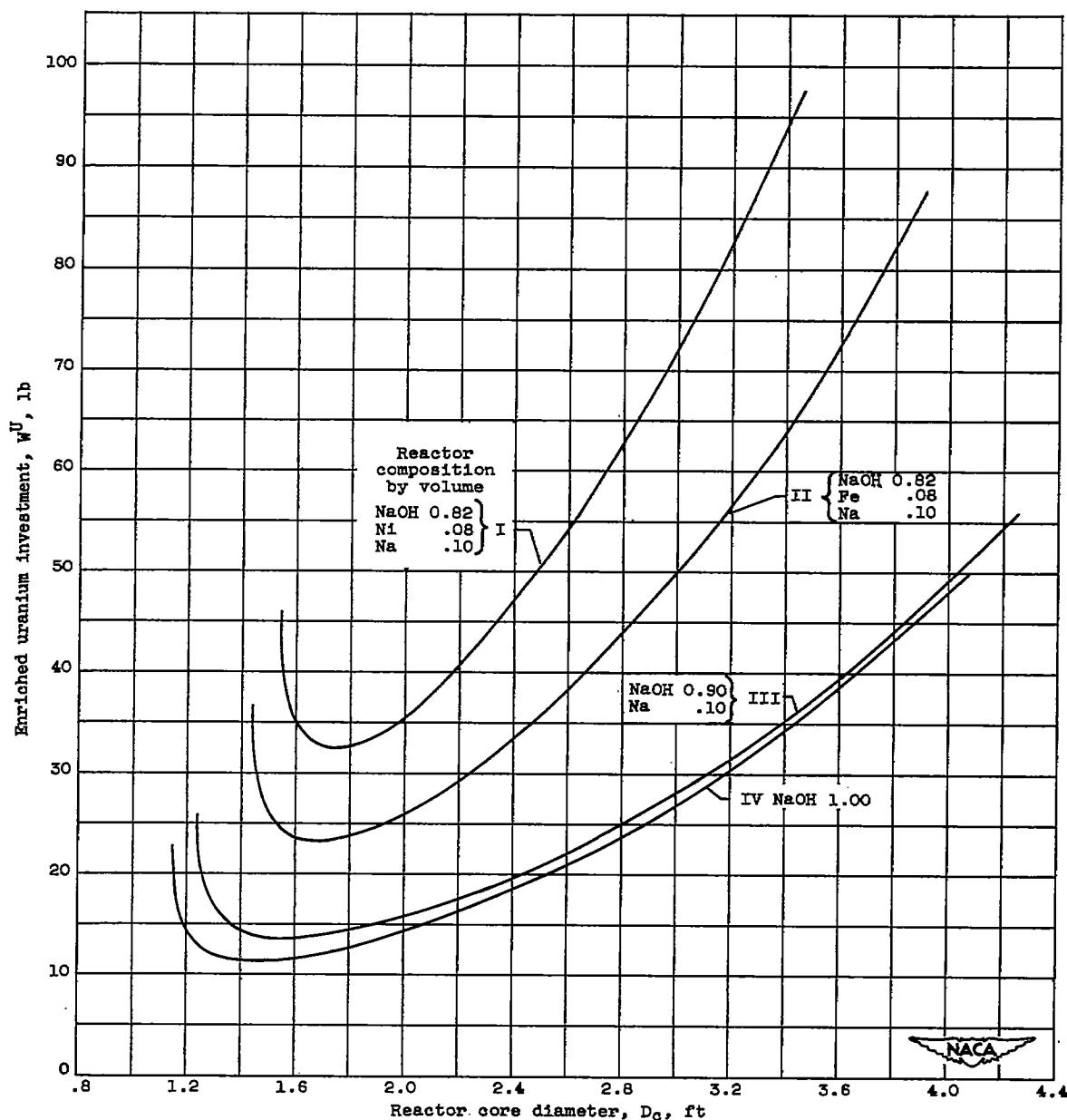
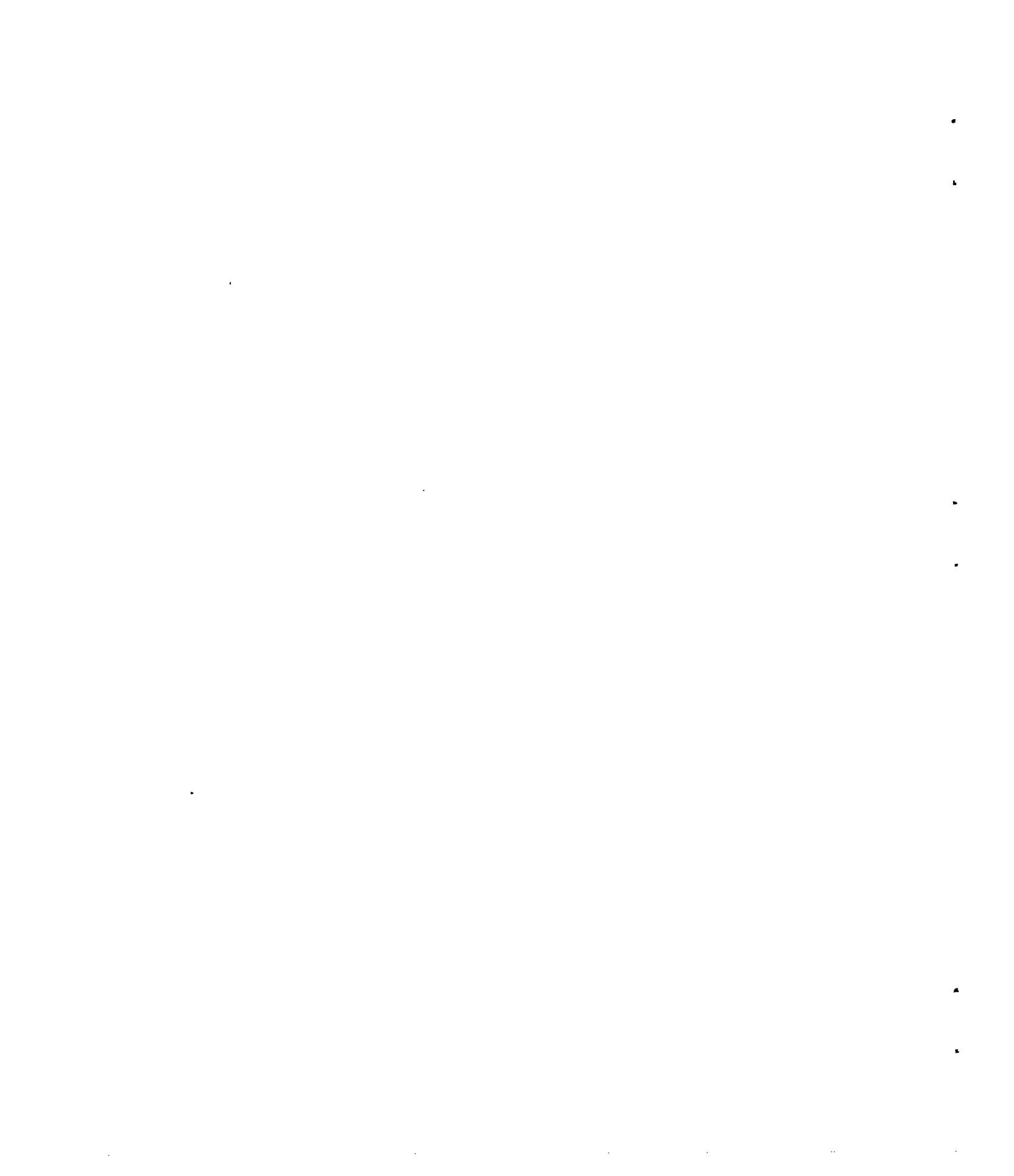


Figure 6. - Comparison of critical reactors I to IV. Reflector thickness, 6 inches of NaOH; length-diameter ratio of cylindrical core, 1.0; average moderator temperature, 1450° F.



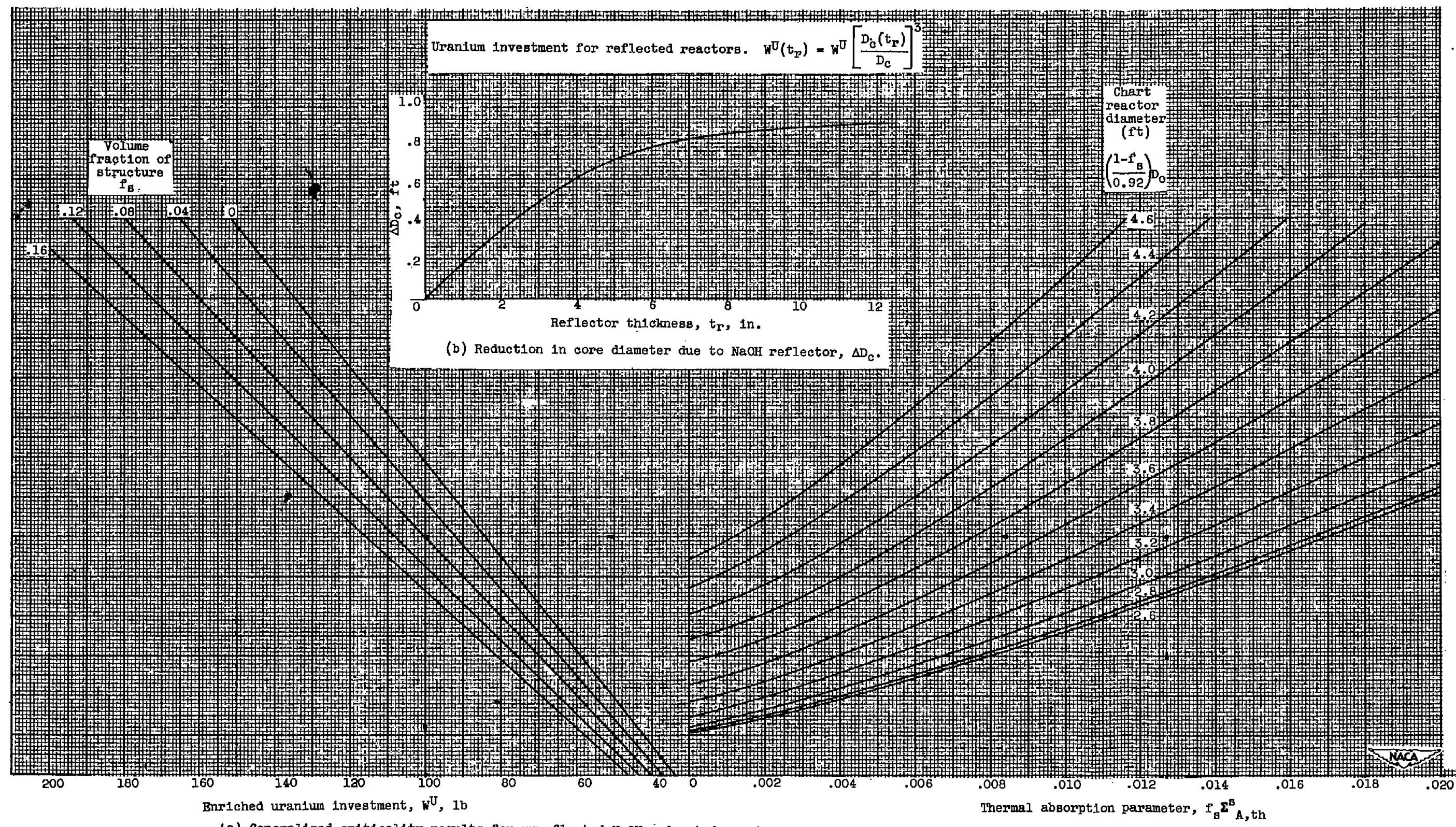
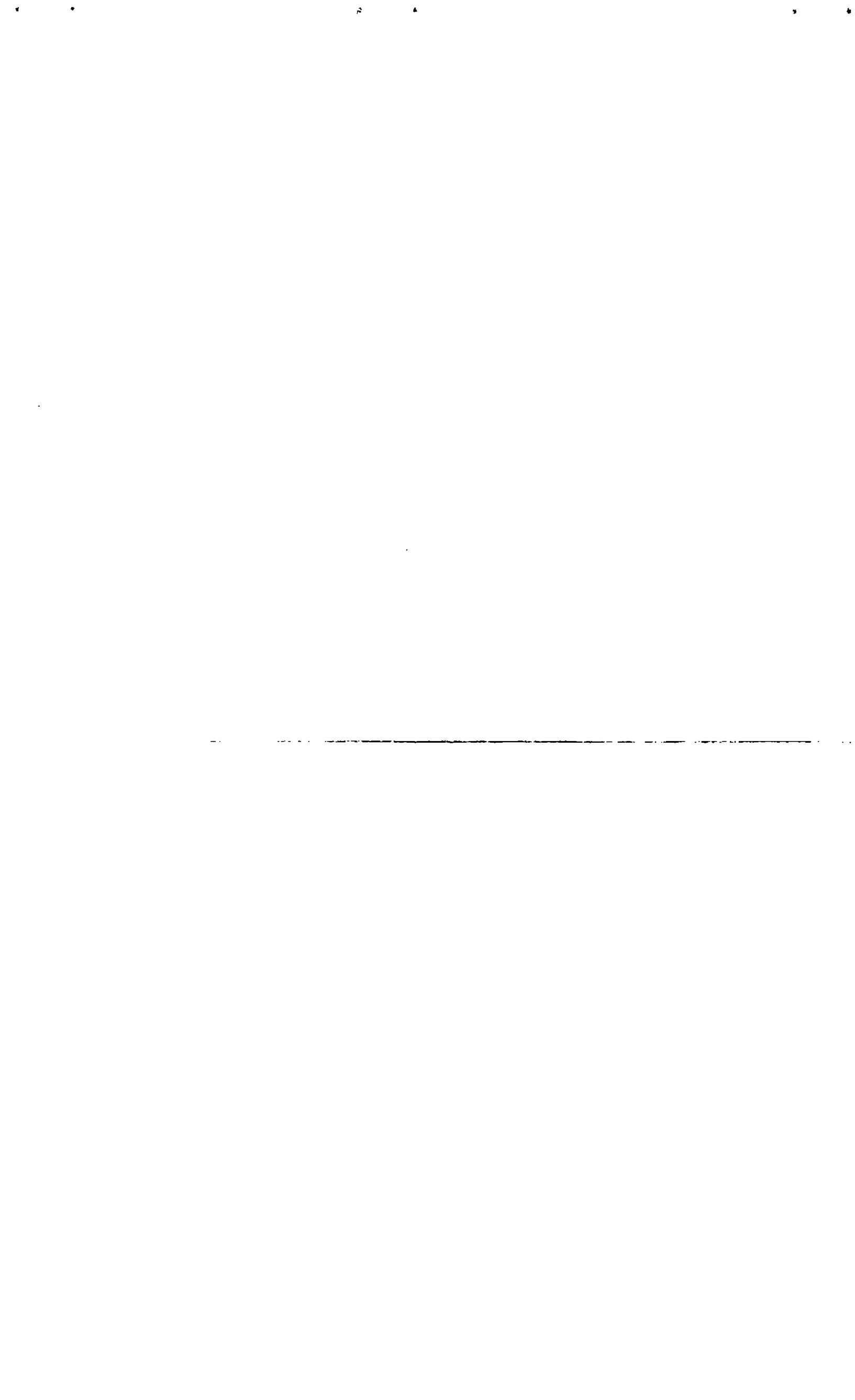
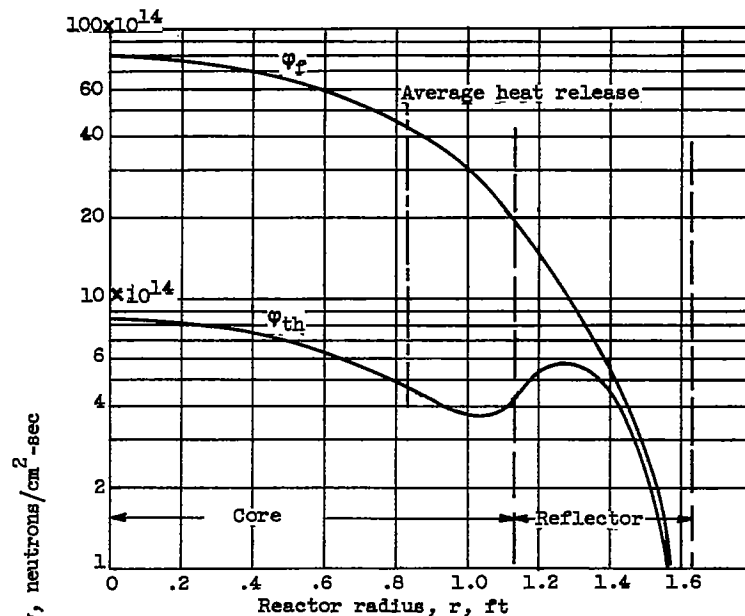
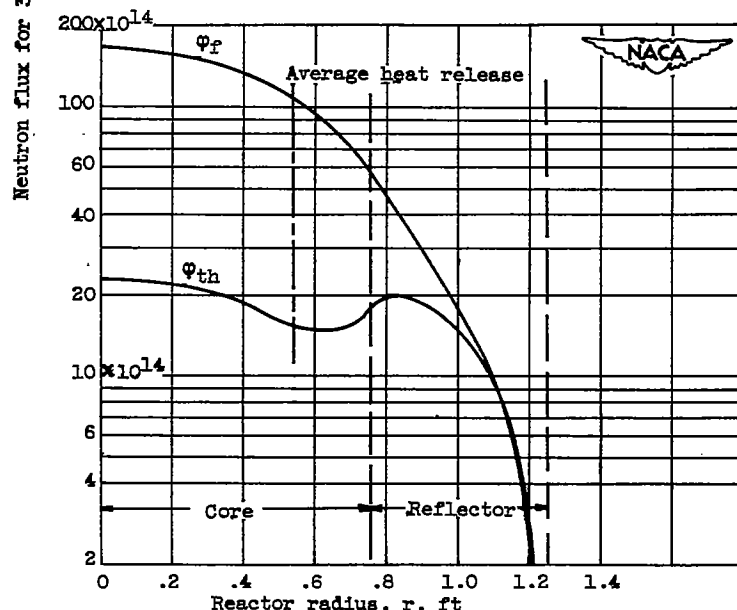


Figure 7. - Generalized critical size and enriched uranium investment as a function of thermal neutron absorption parameter of reactor structure  $f_s \Sigma_{A,\text{th}}^S$  for reactors moderated and reflected by NaOH. Length-diameter ratio of cylindrical core 1.0; average moderator temperature,  $1450^\circ \text{F}$ .





(a) Reactor I. Core composition: NaOH, 0.82;  
Ni, 0.08; Na, 0.10; uranium investment,  
43 pounds.



(b) Reactor III. Core composition: NaOH, 0.90;  
Na, 0.10; uranium investment, 15 pounds.

Figure 8. - Radial neutron flux distributions. Reflector thickness, 6 inches of NaOH; average moderator temperature, 1450°; ratio of hydrogen to uranium atoms R, 100; reactor total heat release, 300,000 kilowatts; flux for total heat release of  $H$  kilowatts given by  $\Phi = \frac{H}{300,000} \Phi_{indicated}$ .

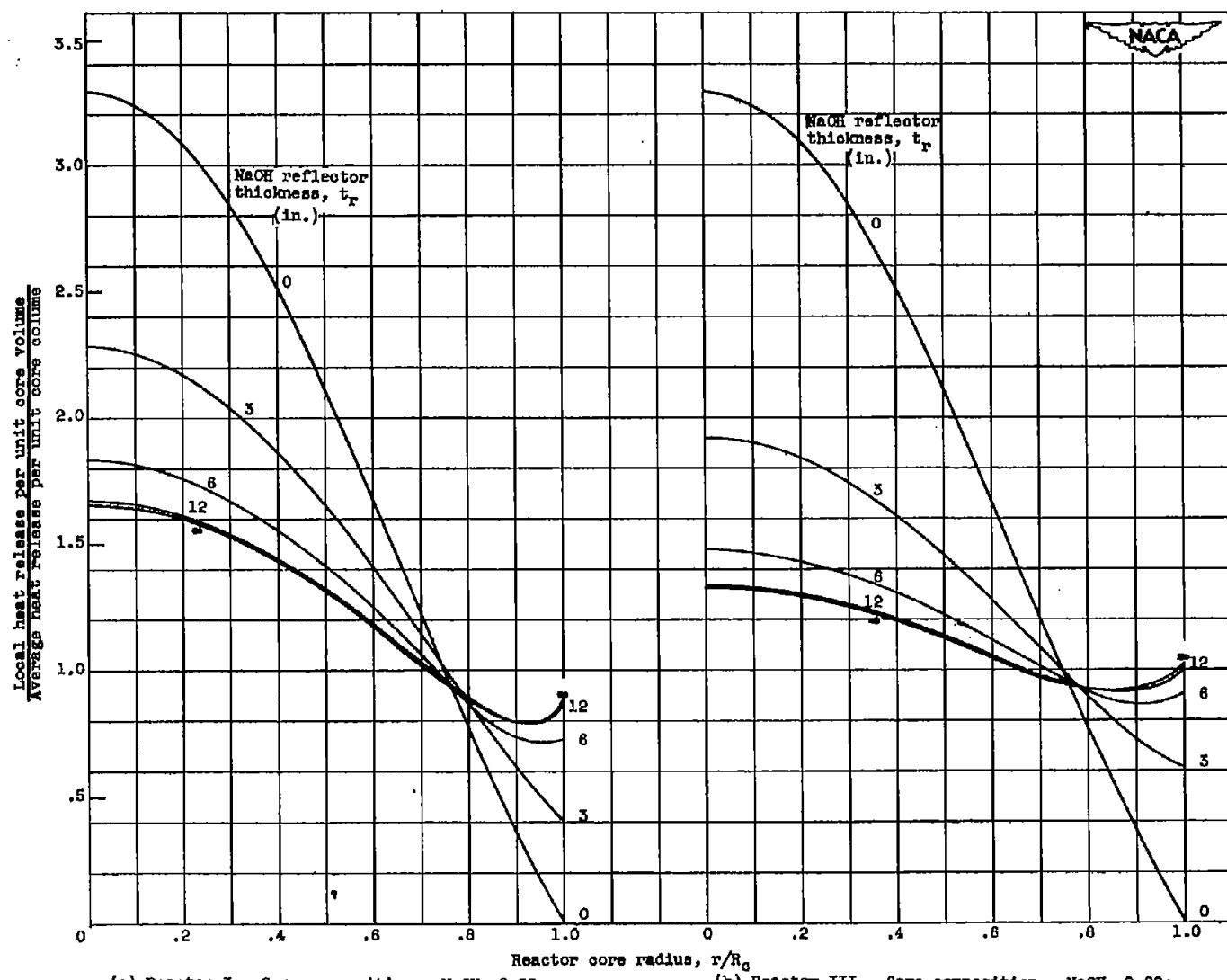
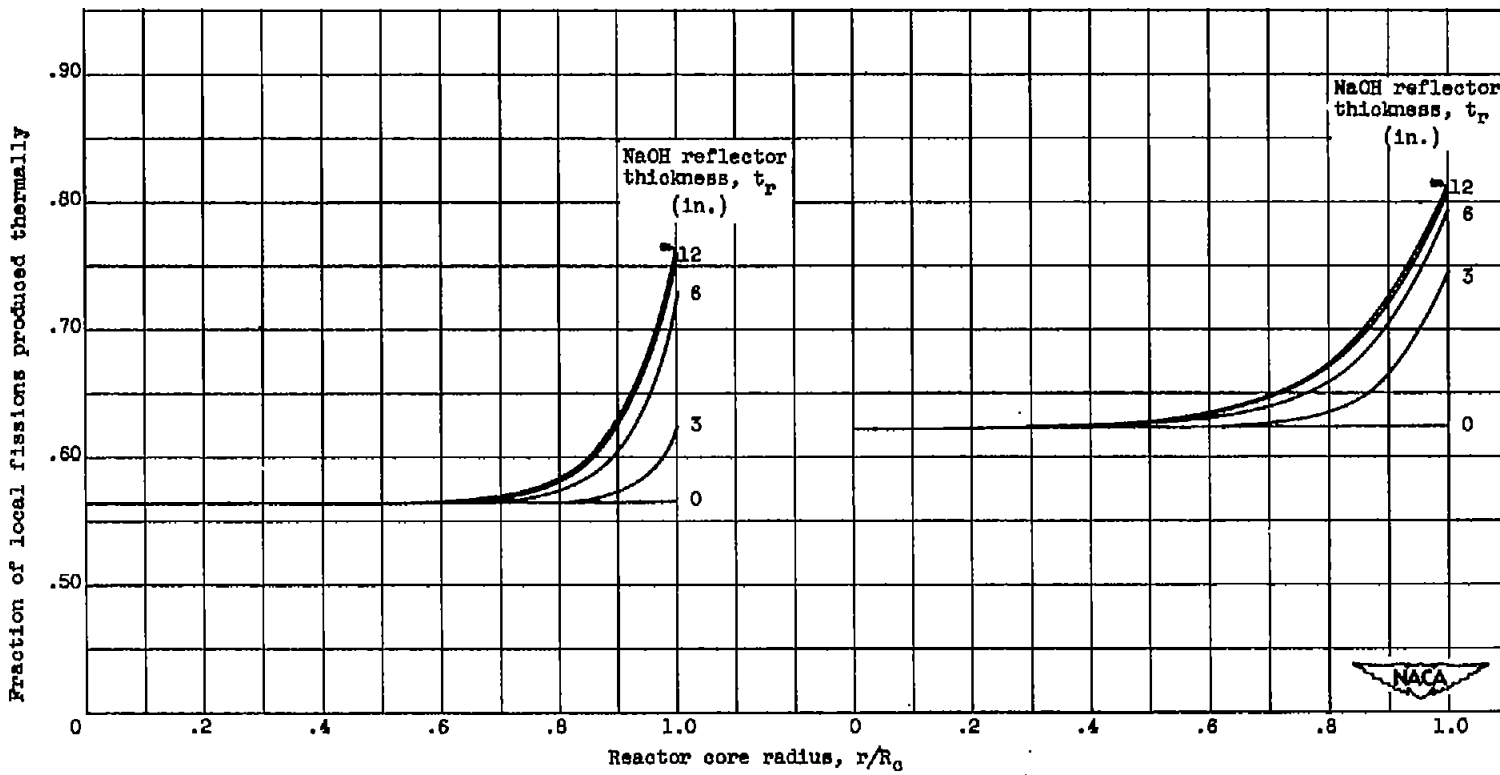


Figure 9. - Radial heat-generation distributions. Thermal temperature,  $1450^{\circ}$  F; ratio of hydrogen to uranium atoms  $R$ , 100.



(a) Reactor I. Core composition: NaOH, 0.82; Ni, 0.08; Na, 0.10.

(b) Reactor III. Core composition: NaOH, 0.90; Na, 0.10.

Figure 10. - Radial distribution of fraction of fissions produced by thermal neutrons. Average moderator temperature, 1450° F; ratio of hydrogen to uranium atoms R, 100.

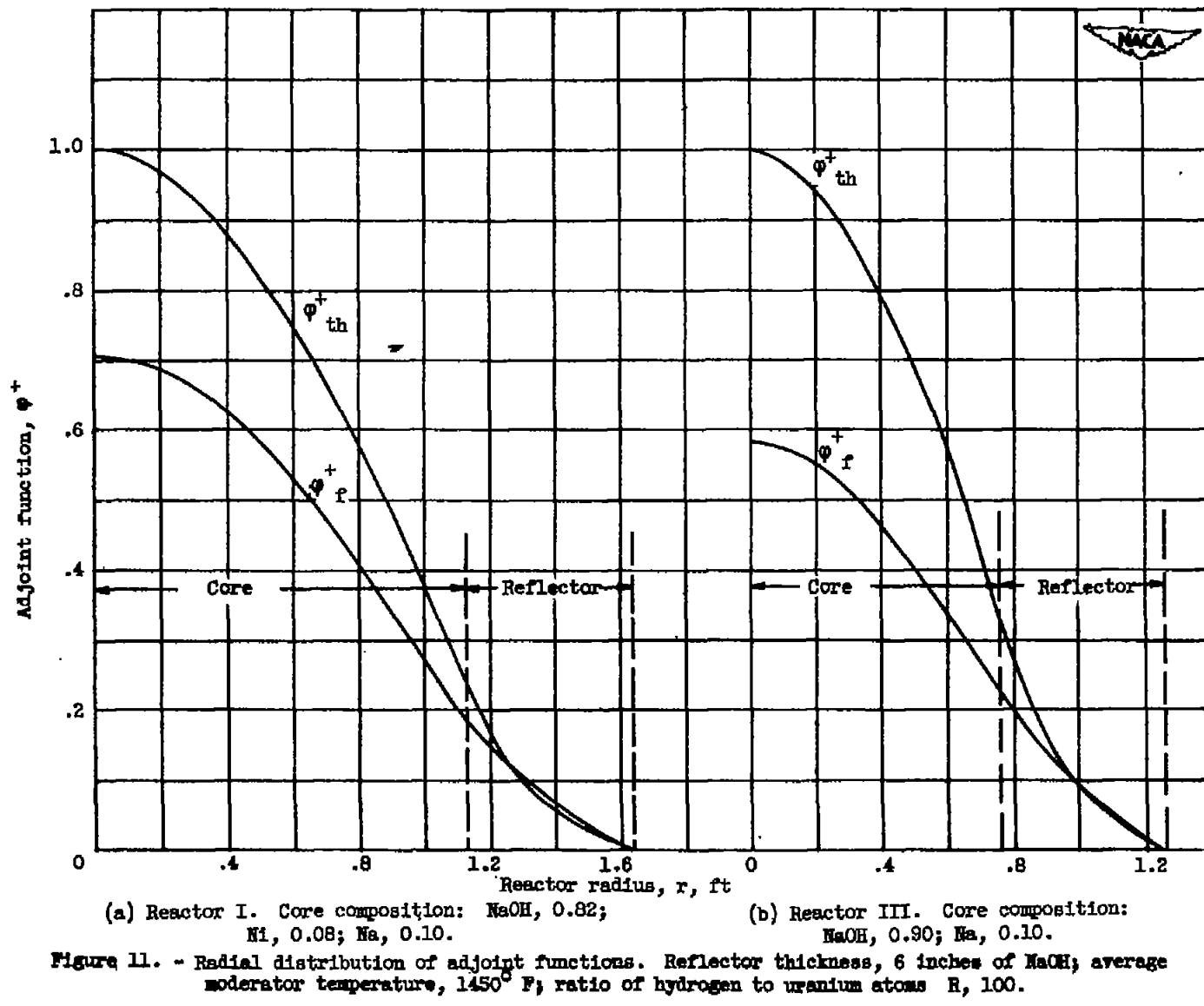


Figure 11. - Radial distribution of adjoint functions. Reflector thickness, 6 inches of NaOH; average moderator temperature, 1450° F; ratio of hydrogen to uranium atoms  $R$ , 100.

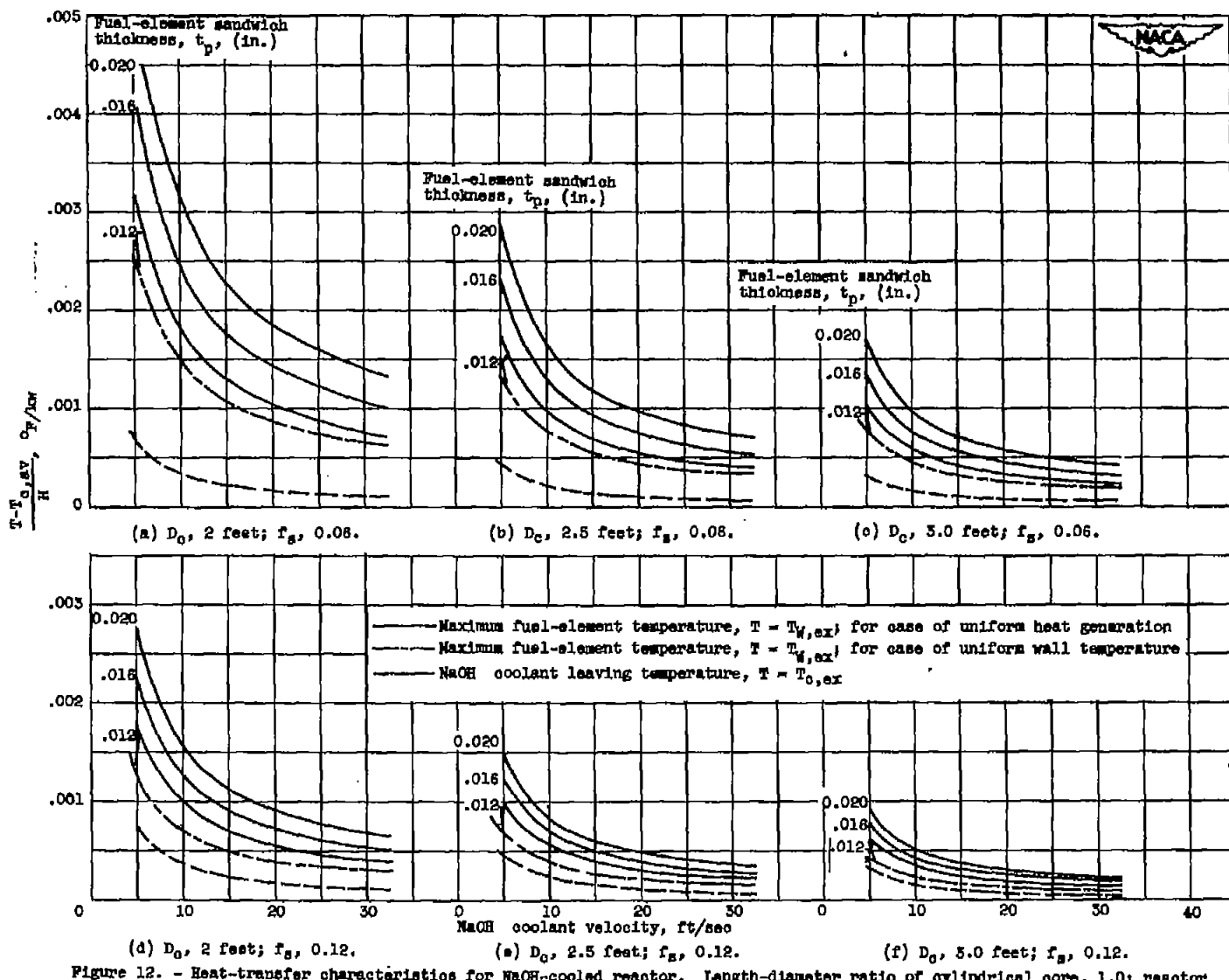


Figure 12. - Heat-transfer characteristics for NaOH-cooled reactor. Length-diameter ratio of cylindrical core, 1.0; reactor core containing plate-type fuel elements (see fig. 1).

2525

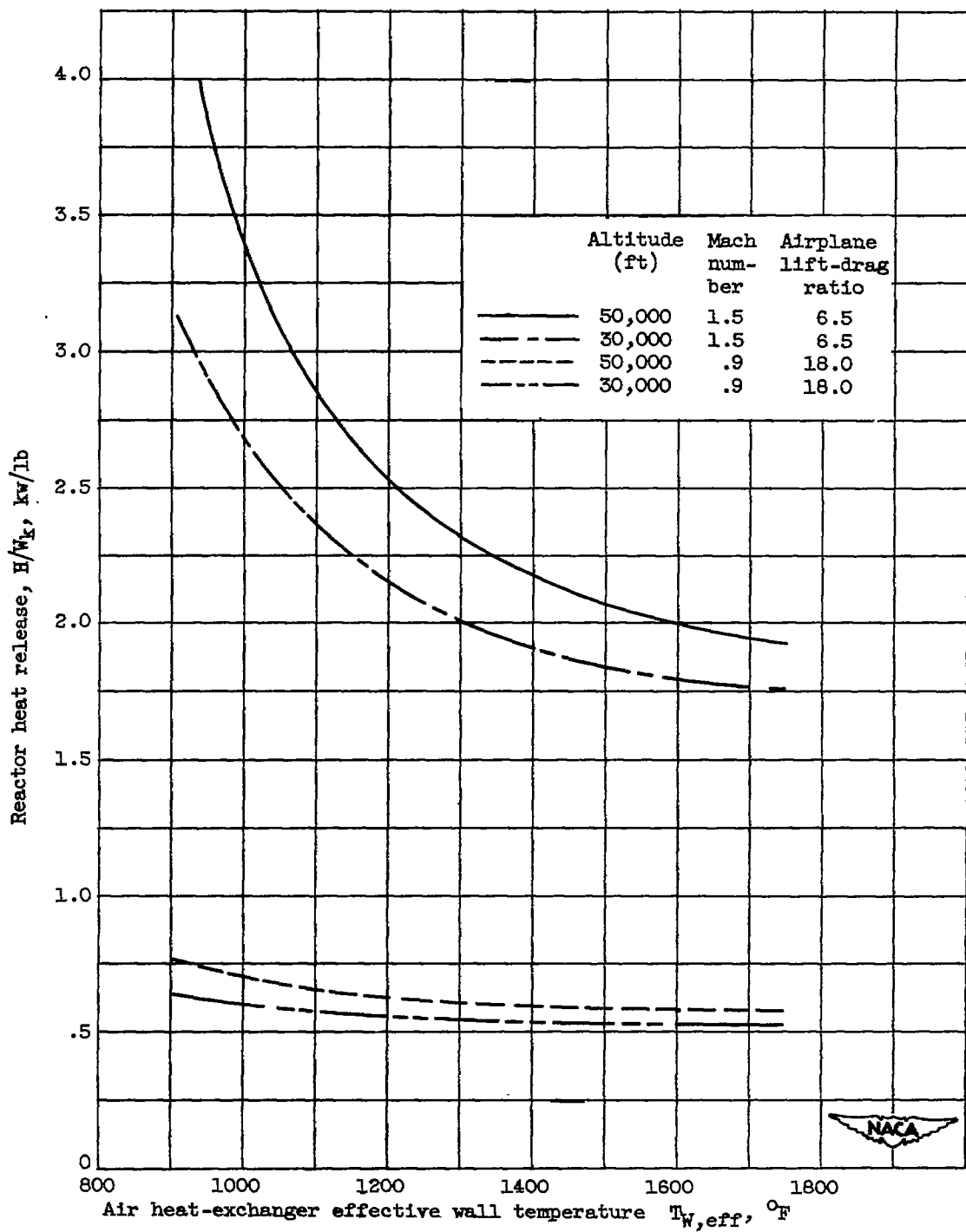


Figure 13. - Variation of required reactor heat release with air heat-exchanger effective wall temperature for optimum turbojet cycle. Data based on reference 14. Ratio of structural to gross weight  $W_s/W_g$ , 0.30.

2525

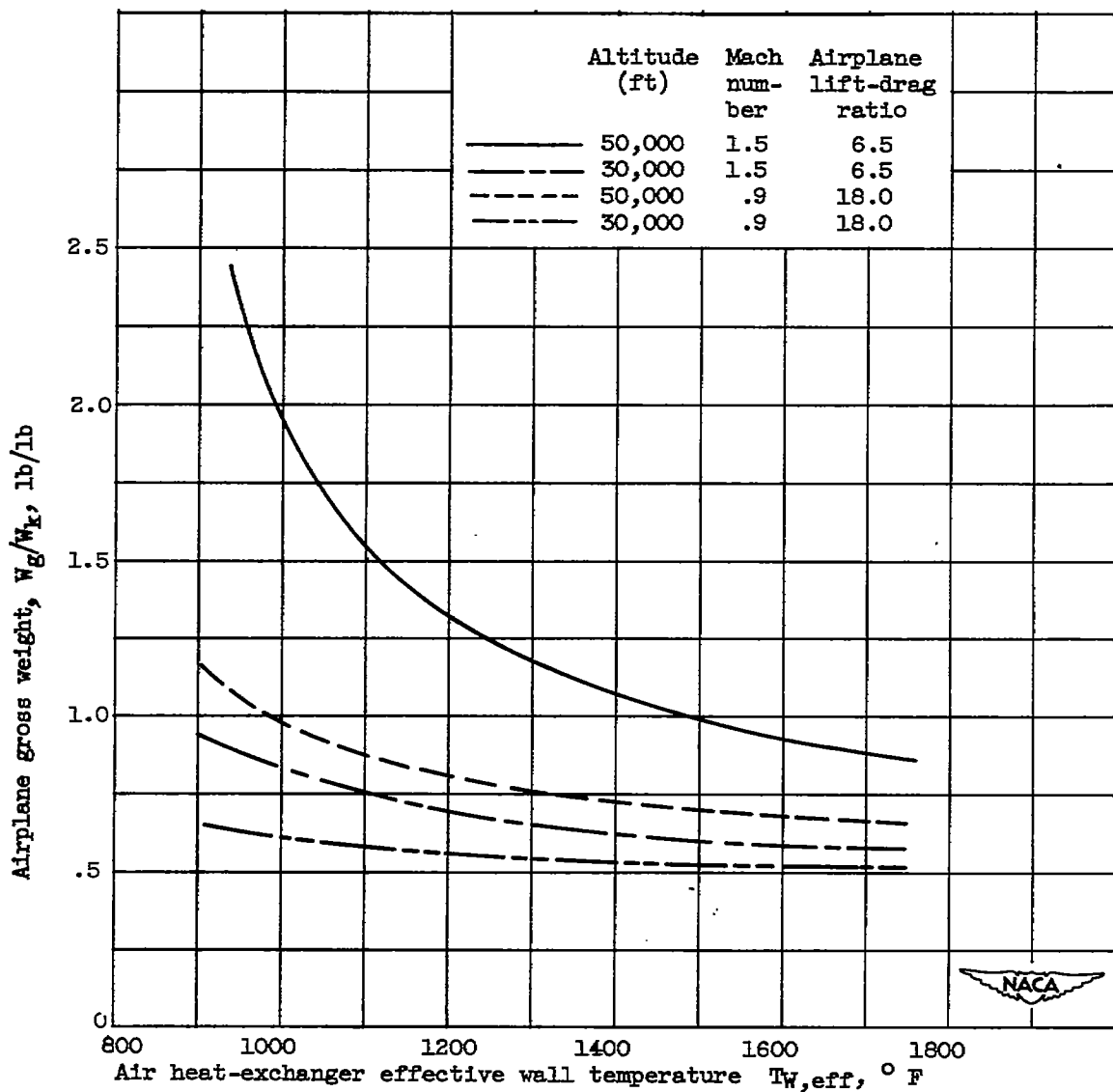


Figure 14. - Variation of required airplane gross weight with air heat-exchanger effective wall temperature for optimum turbojet cycle. Data based on reference 14. Ratio of structural to gross weight  $W_s/W_g$ , 0.30.

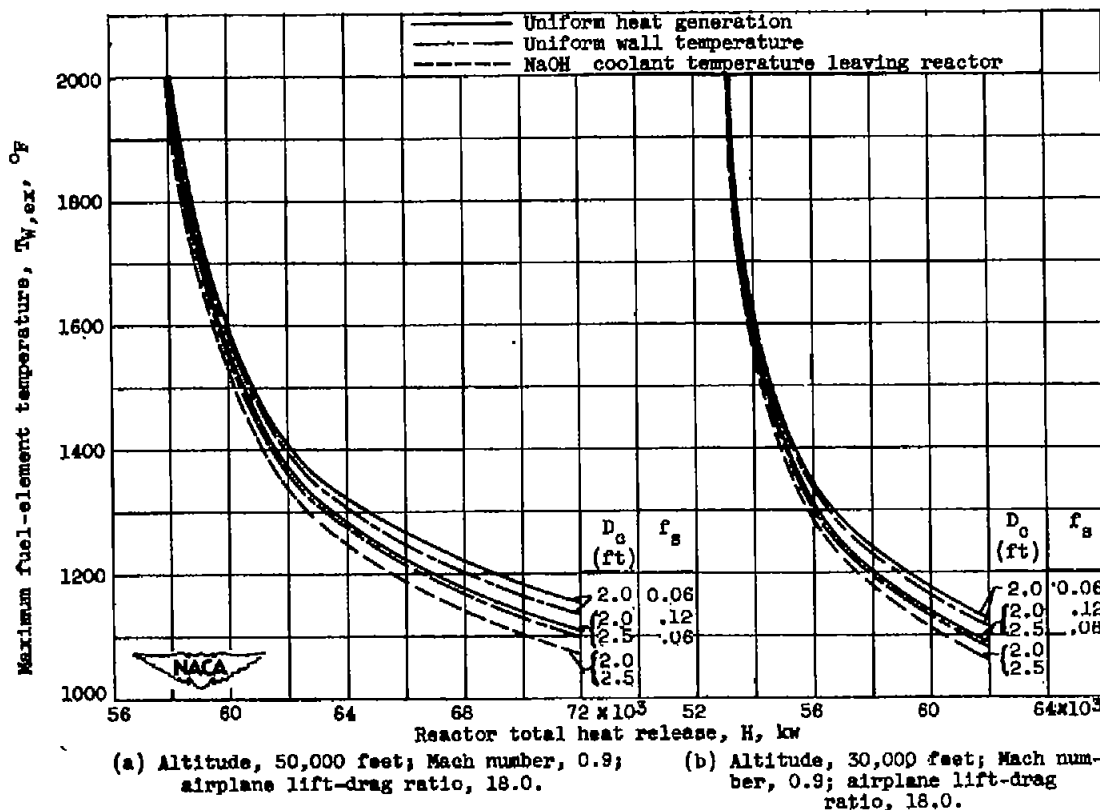
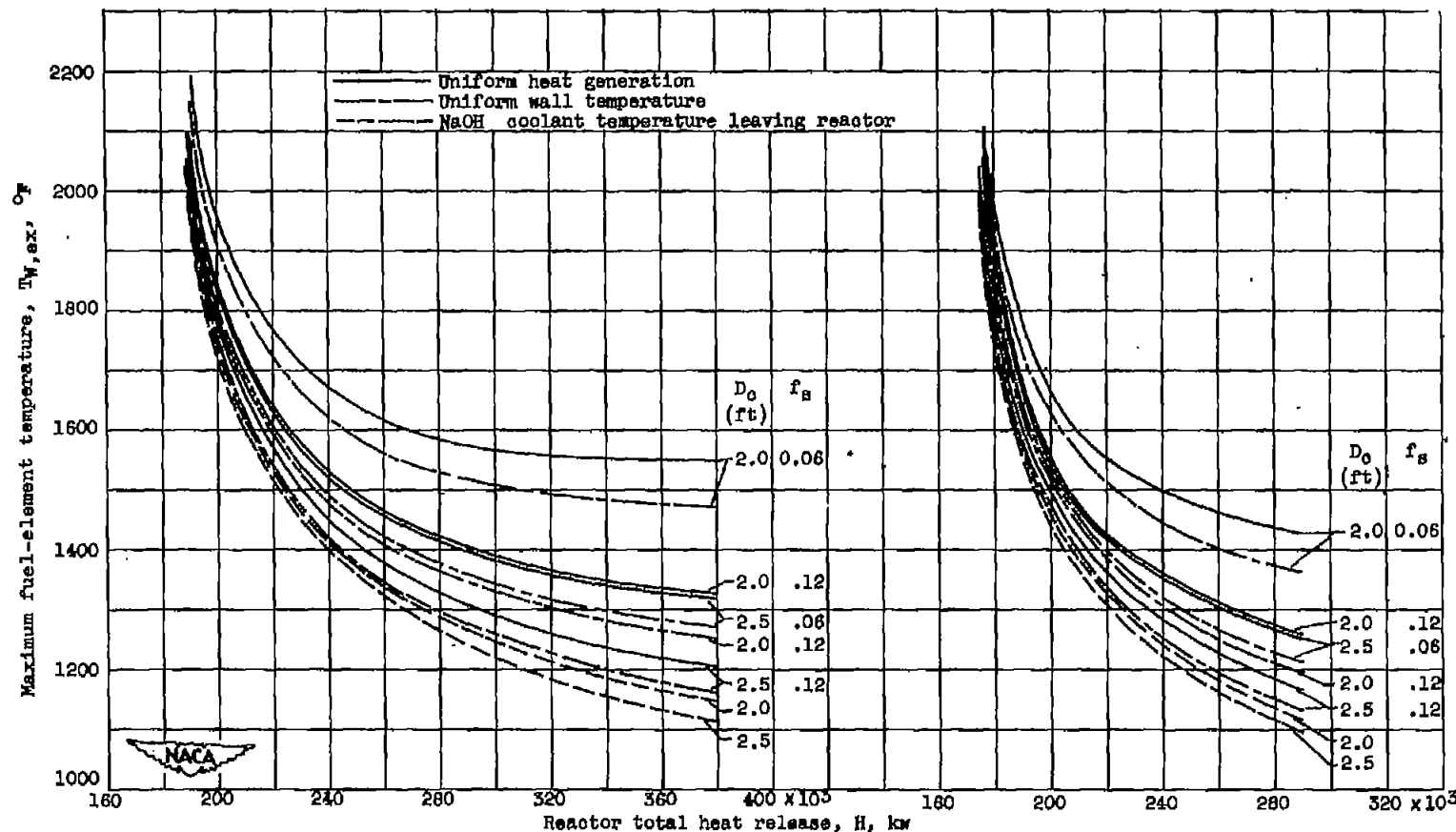


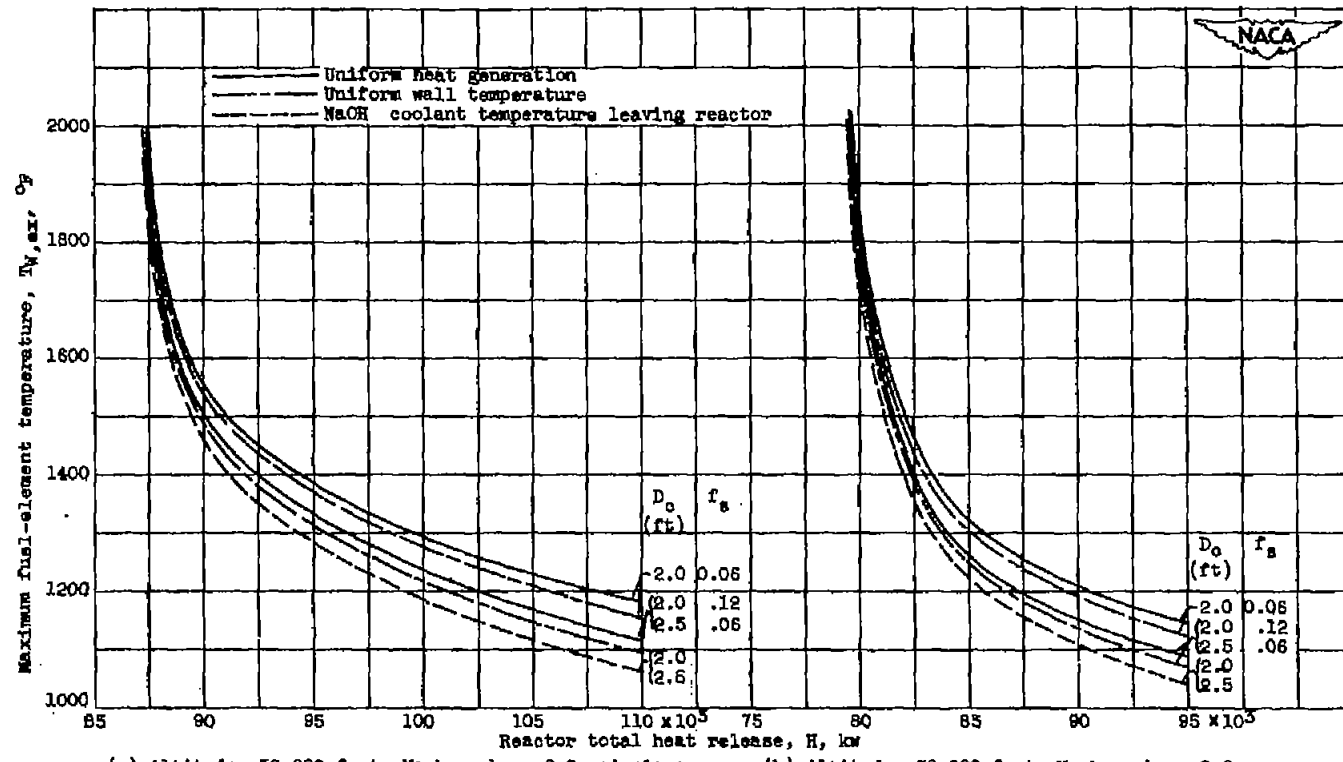
Figure 15. - Maximum fuel-element temperature as a function of required reactor heat release for NaOH-cooled reactors in optimum turbojet cycle. Shield, reactor, pay-load, and auxiliary equipment weight  $W_p$ , 100,000 pounds; ratio of structural to gross weight  $W_s/W_g$ , 0.30; coolant velocity, 15 feet per second; fuel-element sandwich thickness, 0.012 inch; length-diameter ratio of cylindrical core, 1.0.



(c) Altitude, 50,000 feet; Mach number, 1.5; airplane lift-drag ratio, 6.5.

(d) Altitude, 30,000 feet; Mach number, 1.5; airplane lift-drag ratio, 6.5.

Figure 15. - Concluded. Maximum fuel-element temperature as a function of required reactor heat release for NaOH-cooled reactors in optimum turbojet cycle. Shield, reactor, payload, and auxiliary equipment weight  $W_k$ , 100,000 pounds; ratio of structural to gross weight  $W_s/W_g$ , 0.30; coolant velocity, 15 feet per second; fuel-element sandwich thickness, 0.012 inch; length-diameter ratio of cylindrical core, 1.0.



(a) Altitude, 50,000 feet; Mach number, 0.9; airplane lift-drag ratio, 18.0

(b) Altitude, 50,000 feet; Mach number, 0.9; airplane lift-drag ratio, 18.0.

Figure 16. - Maximum fuel-element temperature as a function of required reactor heat release for NaOH-cooled reactors in optimum turbojet cycle. Shield, reactor, pay-load, and auxiliary equipment weight  $W_K$ , 150,000 pounds; ratio of structural to gross weight  $W_S/W_G$ , 0.50; coolant velocity, 15 feet per second; fuel-element sandwich thickness, 0.012 inch; length-diameter ratio of cylindrical core, 1.0.

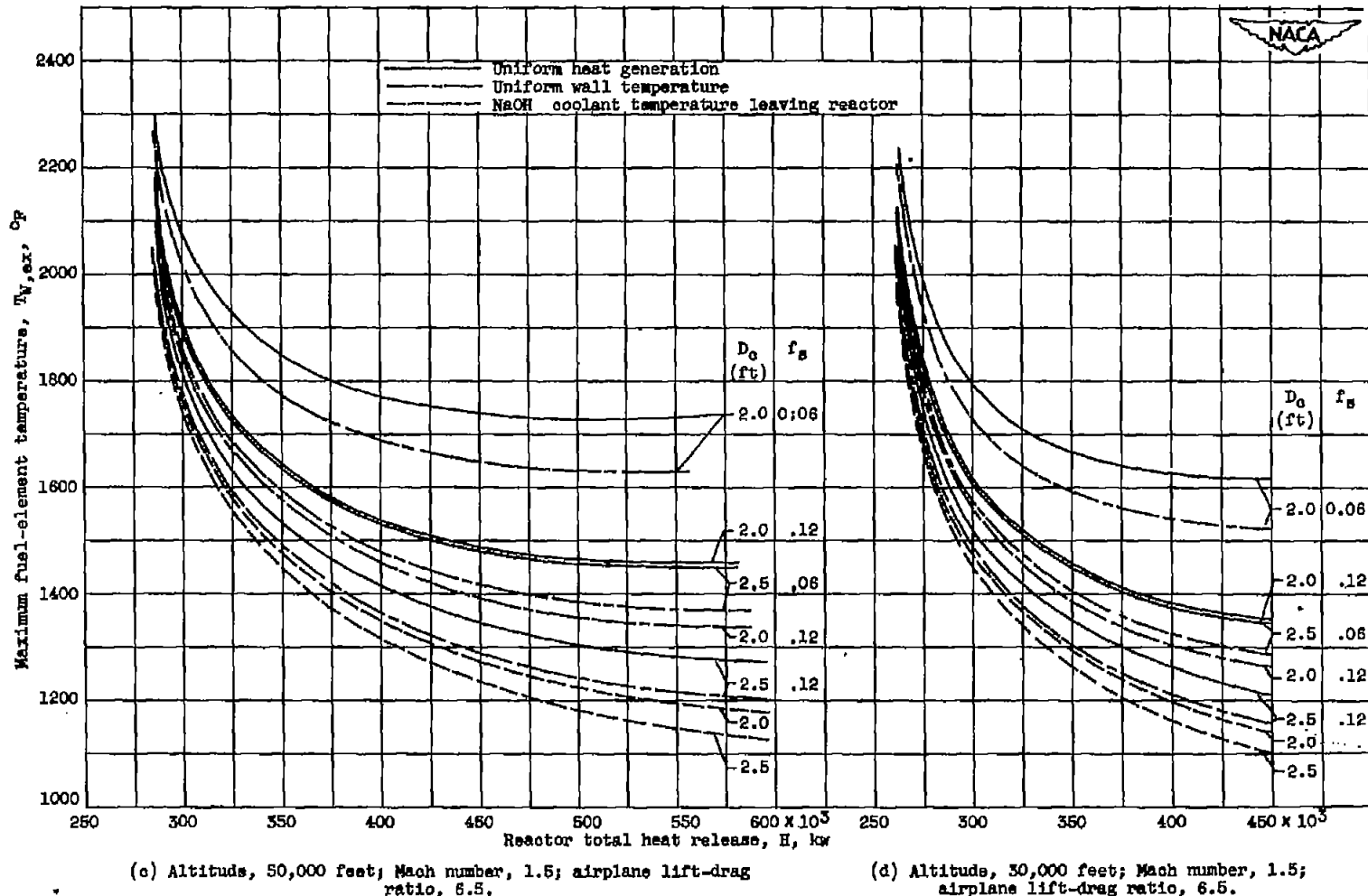


Figure 16. - Concluded. Maximum fuel-element temperature as a function of required reactor heat release for NaOH-cooled reactors in optimum turbojet cycle. Shield, reactor, pay-load, and auxiliary equipment weight  $W_K$ , 150,000 pounds; ratio of structural to gross weight  $W_s/W_g$ , 0.30; coolant velocity, 15 feet per second; fuel-element sandwich thickness, 0.012 inch; length-diameter ratio of cylindrical core, 1.0.

██████████  
SECURITY INFORMATION

NATIONAL ADVISORY COMMITTEE FOR AERONAUTICS

RESEARCH MEMORANDUM

THE SODIUM HYDROXIDE REACTOR: EFFECT OF REACTOR VARIABLES ON CRITICALITY  
AND FUEL-ELEMENT TEMPERATURE REQUIREMENTS FOR SUBSONIC AND  
SUPERSONIC AIRCRAFT NUCLEAR PROPULSION

2525

*Donald Bogart*

Donald Bogart  
Aeronautical Research Scientist  
Propulsion Systems

*Michael F. Valerino*

Michael F. Valerino  
Aeronautical Research Scientist  
Propulsion Systems

Approved:

*Leroy V. Humble*

Leroy V. Humble  
Aeronautical Research Scientist  
Propulsion Systems

*Benjamin Pinkel*

Benjamin Pinkel  
Chief, Material and Thermodynamics  
Research Divisions

cag

██████████  
SECURITY INFORMATION